EFFECT OF OPERATING PARAMETERS ON ELECTROCHEMICAL DEPOSITION OF METALLIC THIN FILMS IN PRESENCE OF ULTRASOUND

THESIS SUBMITTED
IN
PARTIAL FULLFILLMENT OF THE REQUIRMENT FO THE AWARD OF THE DEGREE
OF

Master of Technology
in
Metallurgical and Materials Engineering

Submitted By
Seshadev Sahoo
M.Tech. 4th Semester
Roll No-20604002

DEPT. OF METALLURGICAL AND MATERIALS ENGINEERING
N.I.T ROURKELA

EFFECT OF OPERATING PARAMETERS ON ELECTROCHEMICAL DEPOSITION OF METALLIC THIN FILMS IN PRESENCE OF ULTRASOUND

THESIS SUBMITTED IN PARTIAL FULLFILLMENT OF THE REQUIRMENT FOR THE AWARD OF THE DEGREE OF

Master of Technology
in
Metallurgical and Materials Engineering

Submitted By
Seshadev Sahoo
M.Tech. 4th Semester
Roll No-20604002
DEPT. OF METALLURGICAL AND MATERIALS ENGINEERING
N.I.T ROURKELA

Under the supervision
of

Prof. B.C. Ray
Professor

Prof, (Ms.) Archana Mallick
Lecturer

Dept. of Metallurgical and Materials Engg.
National Institute of Technology, Rourkela
India
769008

National Institute of Technology
Rourkela

CERTIFICATE

This is to certify that the thesis entitled, "EFFECT OF OPERATING PARAMETERS ON ELECTROCHEMICAL DEPOSITION OF METALLIC THIN FILMS IN PRESENCE OF ULTRASOUND" submitted by **Mr. Seshadev Sahoo** in partial fulfillment of the requirements for the award of Master of Technology Degree in **Metallurgical and Materials Engineering** with specialization in **"Metallurgical and Materials Engineering"** at the National Institute of Technology, Rourkela (Deemed University) is an authentic work carried out by him under our supervision and guidance. To the best of our knowledge, the matter embodied in the thesis has not been submitted to any other University / Institute for the award of any Degree or Diploma.

Prof.(Ms.) Archana Mallik
Metallurgical & Materials Engg.
National Institute of technology
Rourkela – 769008

Prof. B.C. Ray
Metallurgical & Materials Engg
National Institute of technology
Rourkela - 769008

Acknowledgement

I avail this opportunity to extend my hearty indebtedness to my guide Prof. B.C Ray, and Prof.(Mrs) Archana Mallik, Metallurgical and Materials Engineering for their valuable guidance constant encouragement and kind help at different stages for the execution of this dissertation work.

I also express my sincere gratitude to, Dr. G.S Aggarwal, HOD, Metallurgical and Materials Engineering for providing valuable departmental facilities.

I am also grateful to Dr.B.B.Verma &Dr.S. Sarkar, M. Tech. coordinator, for his constant concern and encouragement for execution of this work.

I am also thankful to Mr. R. Patnaik, Mr. U. Sahoo, Mr. Sameer Pradhan, Metallurgical & Materials Engineering, Technical assistants, for their help during the execution of experiment.

I am Thankful to The Director of IMMT Bhubaneswar, NML Jamshedpur for their help during the sample characterization.

Special thanks to my friends and other members of the department for being so supportive and helpful in every possible way.

NIT ROURKELA Seshadev Sahoo

CONTENTS

LIST OF FIGURES

LIST OF TABLES

ABSTRACT

Due to their small size and thickness, nanostructured thin films exhibit novel properties which largely differ from the bulk materials. Due to their significant properties it can be used as microelectronic materials, bacteriostatic materials, catalytic materials or magnetorecording materials, antibacterial materials, cryogenic superconducting materials, biosensor materials. Generally the shape, size, and size distribution of particulates and grains can be controlled by adjusting the reaction condition such as external and internal parameters like temperature, electrolyte concentration, current density, P^H of the solution. Sonoelectrochemistry is the study of the effects of the combination of ultrasonic radiation with electrode processes occurring at surfaces of electrodes immersed in a solution in an electrochemical cell. The ultrasound plays an important role to produce cavitation bubbles inside the electrolyte by rupturing the chemical bonds between molecules and electrolyte. The cavitation bubbles implosively collapse within a very short time after undergoing the formation growth and contraction. Synthesis under low temperature may avoid undesirable interdiffusion between adjacent layers and structures and allows uniform modification of surfaces and structures with reduced grain size. In this work we prepare the copper thin film by sonoelectrosynthesis method. The grain size, mechanical and electrical properties of the electrodeposited metal thin film depends upon various parameters like temperature, PH, current density, and concentration of electrolyte and also ultrasound has many numerous effects on the grain size, hardness, porosity and brightness of the deposits. This particle can characterized by XRD, SEM, AFM, DSC and study the mechanical properties by nanaoidentation.

INTRODUCTION

Introduction

Thin films are thin material layers ranging from fractions of a nanometer to several micrometers in thickness. Due to their small thickness, this material exhibit novel properties which largely differ from the bulk materials. They can be used as microelectronic materials, bacteriostatic materials, catalytic materials or magneto recording materials, antibacterial materials, cryogenic superconducting materials biosensor materials [1, 2]. There are many different synthesis methods such as physical vapour deposition, chemical vapour deposition, molecular beam epitaxy, spin coating and electrodeposition. Among these different synthesis method electrochemistry is the most promising method because it offers the advantages of economy, convenience and several experimental parameters can be controlled more precisely [3]. Synthesis under low temperature may avoid undesirable interdiffusion between adjacent layers and structures and allows uniform modification of surfaces and structures with reduced grain size [4]. Sonoelectrochemistry is the study of the effects of the combination of ultrasonic radiation with electrode processes occurring at surfaces of electrodes immersed in a solution in an electrochemical cell. The ultrasound plays an important role to produce cavitation bubbles inside the electrolyte by rupturing the chemical bonds between molecules and electrolyte. The cavitation bubbles implosively collapse within a very short time after undergoing the formation growth and contraction. Collapsing a bubble generates higher temperature than the surrounding and results negative temperature gradient. Higher the negative temperature gradient, smaller the nuclei formed. In this process, metal nuclei are dissolved and deposited on the electrode during electrolysis of electrolyte where as a cavitation effect of ultrasound enhances the nucleation rates of the metal nuclei. [5].

In this work we prepare the metallic thin films by sonoelectrosynthesis method. The electrodeposited metallic thin film depends upon various parameters like temperature, PH, current density, and concentration of electrolyte and also ultrasound has many numerous effects on the grain size, hardness, porosity and brightness of the deposited thin film. Hence an attempt has been made to observe the above mentioned effects in presence of ultrasound. Experimentation was done with a temperature range of 25˚C, 20˚C, 15˚C,

10˚C, 5˚C, − 1˚C, − 3˚C at a particular concentration of copper and acid. To experiment with metal ion concentration the range chosen are 10 g l $^{-}$1, 20 g l $^{-}$1, 30 g l $^{-}$1, 40 g l $^{-}$1 and 50 g l $^{-}$1. and for acid concentration effects the range is 40 g l $^{-1}$ – 120 g l $^{-}$1 at an interval of 20 g l $^{-1}$. structural and phase analysis of the films are characterized by XRD. Microstructural surface analysis are mainly done by SEM and AFM. The analysis confirms the nano range deposit with decreasing temperature, increasing acid concentration and copper concentration. Mechanical properties are done by nano indentation tests. The result shows an increase in hardness values with decreased temperature. Specific heat of the sample are done by DSC. It supports the fact from microstrutural analysis that the deposits are in nano regime as there is in increase in heat capacity with decreasing size. The work needs further amplification to explore the electrochemistry in presence of ultrasound with various parameters.

Chapter-1

Literature Review

CHAPTER 1

1. Literature Review

1.1Thin film Technology

A solid material is said to be a thin film form when it is built up, as a thin layer on a solid support, called substrate, ab initio by controlled condensation of the individual atomic, molecular, or ionic species, either directly by a physical process, or via a chemical and/or electrochemical reaction. Since individual atomic, molecular, or ionic species of matter may exist either in the vapour or in the liquid phase, the techniques of thin film deposition can be broadly classified under two main categories :(1) vapour phase deposition and (2) liquid-phase /solution deposition. Films prepared by direct application of a dispersion or a paste of the material on a substrate , and letting it dry , are called irrespective of their thickness , thick films and have characteristically different from those of the thin films[6].

In thin films, deviations from the properties of the corresponding bulk materials arise because of their small thickness, large surface-to-volume ratio, and unique physical structure which is a direct consequence of the growth process. Some of the phenomena arising as a natural consequence of small thickness are optical interference , electronic tunneling through an insulating layer , high resistivity and low temperature coefficient of resistance , increase in critical magnetic field and critical temperature of superconductor , the Josephson effect, and planar magnetization. The high surface to volume ratio of thin films due to their small thickness and microstructure can influence a number of phenomena such as gas adsorption, diffusion, and catalytic activity. Similarly enhancement of superconducting transition temperature, corrosion resistance, hardness, thermopower and optical absorption arises in thin films of certain materials having metastable disordered structures [7].

1.2. Properties and application of thin films

1.2.1. Mechanical effects in Thin Films

Thin films are unusual specimens for the study of mechanical effects in materials in the presences of a high internal structural disorder.Vapour-deposited films are generally under enomorous stresses (10^9 to 10^{10} dynes/cm^2) and further contain a high density of lattice defects which, even in most cases of epitaxial films, amount to 10^{11} dislocations/cm^2.The level of the intrinsic stress is comparable with the yield strength of many bulk materials and should have a strong influence on the physical and mechanical stability and the properties of the films. The high density of defects and the presences of free surface make it difficult to generate or move dislocations in a film. This condition results in the enhancement of the tensile strength of films up to 200 times the value in the corresponding bulk material.

The use of thin films for modification of engineering surfaces for protection of machine components and devices from enviourmental effects and mechanical damage, thus increasing their life and/or enhancing their aesthetic appeal. It is convenient to classify the various surface engineering applications in to three main categories (1) surface passivation application-those involving from enviourmental effects, (2) tribological applications-those involving protection from mechanical damage and (3) decorative applications [6, 7].

1.2.2. Transport Phenomena in Thin films

Electronic properties of films have been largely stimulated by many attractive microelectronic device applications. Because of surface scattering of carriers in films of thickness comparable with the mean free path, the electrical and thermal transport properties of metals and semiconductors are modified. This modification, called the size effect depends on the ratio of the film thickness to mean free path, which may be varied by changing the film thickness and temperature, and by applying a magnetic field. Due to there electronic properties it is used as Thin film passive component like resistor, capacitor, inductor and thin film active components like thin film transistor, thin film diode, thin film integrated circuit, charge-coupled device, thin film strain gauges and gas sensor etc. [6,7].

1.2.3. Superconductivity in films

Films of thickness comparable with the penetration depth and coherence length of a superconductor are ideal specimens for studying the superconducting behavior of type I and

type II superconductors in the light of various theories. Such studies have played a major role in the theoretical understanding of superconductivity and have made it possible to determine the superconductivity parameters of penetration depth, coherence length and the Ginzburg-Landue coupling constant. When a dc potential appears across a Josephson junction, microwave photons of definite frequency are emitted.Conversly the absorption of such microwave produces the supercurrent.A Josephson tunnel junction therefore act as an emitter and detector of microwaves.

The zero resistance state of a superconductor can be transformed reversible to the finite resistance state, or switched to another part of the superconducting circuit by means of suitable current or a magnetic field forms the basic principle of a verity of promising superconductive devices like computer memory device, crytron Amplifiers, superconductive Tunneling device and SQUIDs etc.[6,7,8].

1.2.4. Ferromagnetism in thin films

The uniqueness of the thin film ferromagnetic phenomena is due to the geometry and microstructure of films. Owing to the pinning of an increasing number of spins at the surface of a ferromagnetic film, the saturation magnetization decreases rapidly below about 30A$^{\circ}$ thickness. The surface pinning makes it possible to excite spin waves across the film thickness, an interesting phenomenon which yields a direct measurement of the ferromagnetic exchange constant. The planar geometry of a ferromagnetic film produces a very high demagnetizing field perpendicular to the plane as compared with that in the plane of the film. This anisotropy becomes uniaxial when the film is deposited in the presences of a magnetic field so that the magnetization is aligned wit the field direction. This direction of magnetization can be reversed to the energetically equivalent direction in very short time by means of small magnetic field .This switching process is the attractive feature for computer applications like Flat film memory, Magneto-optical memory,Ferroacoustic Memory, Domain Motion device, Thin film magnetic Heads, Magnetic Displays etc.[8].

1.3. Thin Film Deposition

Thin-film deposition is any technique for depositing a thin film of material onto a substrate or onto previously deposited layers. "Thin" is a relative term, but most deposition

techniques allow layer thickness to be controlled within a few tens of nanometers, and some allow single layers of atoms to be deposited at a time [6,7].

It is useful in the manufacture of optics (for reflective or anti-reflective coatings, for instance), electronics (layers of insulators, semiconductors, and conductors form integrated circuits), packaging (i.e., aluminum-coated PET film), and in contemporary art.

Deposition techniques fall into two broad categories, depending on whether the process is primarily chemical or physical. These are

1-Physical deposition

2-Chemical deposition

3-Other deposition

1.3.1. Physical deposition

Physical deposition uses mechanical or thermodynamic means to produce a thin film of solid. An everyday example is the formation of frost. Since most engineering materials are held together by relatively high energies, and chemical reactions are not used to store these energies, commercial physical deposition systems tend to require a low-pressure vapor environment to function properly; most can be classified as Physical vapor deposition or PVD [9].

The material to be deposited is placed in an energetic, entropic environment, so that particles of material escape its surface. Facing this source is a cooler surface which draws energy from these particles as they arrive, allowing them to form a solid layer. The whole system is kept in a vacuum deposition chamber, to allow the particles to travel as freely as possible. Since particles tend to follow a straight path, films deposited by physical means are commonly directional, rather than conformal.

Physical deposition includes:

- A **thermal evaporator** uses an electric resistance heater to melt the material and raise its vapor pressure to a useful range. This is done in a high vacuum, both to allow the vapor to reach the substrate without reacting with or scattering against other gas-phase atoms in the chamber, and reduce the incorporation of impurities from the residual gas in the vacuum chamber. Obviously, only materials with a much higher vapor pressure than the heating element can be deposited without contamination of

the film. Molecular beam epitaxy is a particular sophisticated form of thermal evaporation.

- An **electron beam evaporator** fires a high-energy beam from an electron gun to boil a small spot of material; since the heating is not uniform, lower vapor pressure materials can be deposited. The beam is usually bent through an angle of 270° in order to ensure that the gun filament is not directly exposed to the evaporant flux. Typical deposition rates for electron beam evaporation range from 1 to 10 nanometers per second.
- **Sputtering** relies on a plasma (usually a noble gas, such as Argon) to knock material from a "target" a few atoms at a time. The target can be kept at a relatively low temperature, since the process is not one of evaporation, making this one of the most flexible deposition techniques. It is especially useful for compounds or mixtures, where different components would otherwise tend to evaporate at different rates. Note, Sputtering step coverage is more or less conformal.
- **Pulsed laser deposition** systems work by an ablation process. Pulses of focused laser light vaporize the surface of the target material and convert it to plasma; this plasma usually reverts to a gas before it reaches the substrate.
- **Cathodic Arc Deposition** or Arc-PVD which is a kind of ion beam deposition where an electrical arc is created that literally blasts ions from the cathode. The arc has an extremely high power density resulting in a high level of ionization (30-100%), multiply charged ions, neutral particles, clusters and macro-particles (droplets). If a reactive gas is introduced during the evaporation process, dissociation, ionization and excitation can occur during interaction with the ion flux and a compound film will be deposited.

1.3.2. Chemical deposition

In this process, fluid precursor undergoes a chemical change at a solid surface, leaving a solid layer. An everyday example is the formation of soot on a cool object when it is placed inside a flame. Since the fluid surrounds the solid object, deposition happens on every surface, with little regard to direction; thin films from chemical deposition techniques tend to be conformal, rather than directional [10].

Chemical deposition is further categorized by the phase of the precursor:

- **Plating** relies on liquid precursors, often a solution of water with a salt of the metal to be deposited. Some plating processes are driven entirely by reagents in the solution (usually for noble metals), but by far the most commercially important process is electroplating. It was not commonly used in semiconductor processing for many years, but has seen resurgence with more widespread use of Chemical-mechanical polishing techniques.
- **Chemical Solution Deposition** (CSD) uses a liquid precursor, usually a solution of organ metallic powders dissolved in an organic solvent. This is a relatively inexpensive, simple thin film process that is able to produce stoichiometrically accurate crystalline phases.
- **Chemical vapor deposition** (CVD) generally uses a gas-phase precursor, often a halide or hydride of the element to be deposited. In the case of MOCVD, an organometallic gas is used. Commercial techniques often use very low pressures of precursor gas.
- **Plasma enhanced CVD** uses an ionized vapor, or plasma, as a precursor. Unlike the soot example above, commercial PECVD relies on electromagnetic means (electric current, microwave excitation), rather than a chemical reaction, to produce a plasma.

1.3.3. Other deposition processes

Some methods fall outside these two categories, relying on a mixture of chemical and physical means:

- **Molecular beam epitaxy** (MBE), slow streams of an element can be directed at the substrate, so that material deposits one atomic layer at a time. Compounds such as gallium arsenide are usually deposited by repeatedly applying a layer of one element (i.e., Ga), then a layer of the other (i.e., As), so that the process is chemical, as well as physical. The beam of material can be generated by either physical means (that is, by a furnace) or by a chemical reaction (chemical beam epitaxy) [11].
- **Spin coating** is a procedure used to apply uniform thin films to flat substrates. In short, an excess amount of a solution is placed on the substrate, which is then rotated at high speed in order to spread the fluid by centrifugal force. A machine used for spin coating is called a spin coater, or simply spinner. Rotation is continued while the

fluid spins off the edges of the substrate, until the desired thickness of the film is achieved. The applied solvent is usually volatile, and simultaneously evaporates. So, the higher the angular speed of spinning, the thinner the film. The thickness of the film also depends on the concentration of the solution and the solvent. Spin coating is widely used in micro fabrication, where it can be used to create thin films with thicknesses below 10 nm. It is used intensively in photolithography, to deposit layers of photoresist about 1 micrometer thick. Photoresist is typically spun at 20 to 80 Hz for 30 to 60 seconds [12].

1.4. Electrochemistry in Thin Film Technology

Electrochemistry is a key technology in Thin film Technology. Electroplating offers novel routes to ultrafine particles via arrested and templated electrodeposition. As the science underlying the preparation and assembly of ultrafine particles matures methods of exploiting the novel properties of these new functional materials are being scrutinised. Electrochemistry is a suitable method for coupling particle activity to external circuitry.

Electrochemistry is a branch of chemistry that studies chemical reactions which take place at the interface of an electron conductor (the electrode composed of a metal or a semiconductor , including graphite) and an ionic conductor(the electrolyte) and which involve electrone transfer between the electrode and the electrolyte.

If a chemical reaction is caused by an external voltage, as in electrolysis, or if a voltage is caused by a chemical reaction, as in a battery, it is an electrochemical reaction. Chemical reactions where electrons are transferred between atoms are called oxidation/reduction (redox) reaction. In general, electrochemistry deals with situations where oxidation and reduction reactions are separated in space, connected by an external electric circuit.

Electrochemical processes are redox reactions where energy is produced by a spontaneous reaction which produces electricity. In a redox reaction an atoms or ions oxidation state changes as a result of an electron transfer.

The elements involved in an electrochemical reaction are characterized by the number of electrons each has. The oxidation state of an ion is the number of electrons it has accepted or donated compared to its neutral state. If an atom or ion donates an electron in a reaction its

oxidation state is increased, if an elements accepts an electron its oxidation state is decreased. In general, oxidation and reduction always occur in a paired fashion such that one species is oxidized when another is reduced. A reaction in which both oxidation and reduction is occurring is called a redox reaction.

The loss of electron of a substance is called oxidation and the gain of electrons is reduction. The substance which losses electron is known as reducing agent or reductant and the substance which accepts the electron is called the oxidizing agent or oxidant [13, 14]

1.4.1. Electrochemical deposition

Electrochemical metal deposition is one of the oldest subjects within the framework of electrochemistry. Metal electrodeposition takes place at electrode: electrolyte interfaces under the influence of an electric field. The occurrence of chemical changes due to passage of electric current through an electrolyte is termed as electrolysis and the deposition of any substance on an electrode as a consequence of electrolysis is called electrodeposition.

The phenomenon of electrolysis is governed by the following two laws, first enunciated by faraday in 1933: (1) The magnitude of the chemical change occurring is proportional to the electricity passed. (2) The masses of different species deposited at or dissolved from the electrodes by the same quantity of electricity are in proportional to their chemical equivalent weights.

When a metal M is dipped in a solution of its own ions, a dynamic equilibrium

$$M \rightarrow M^{+n} + ne \qquad (1)$$

is set up, as a consequence of which a resultant potential, develops between the electrode and the electrolyte, in the absence of an eternal voltage. The electrode thus gains a certain charge on its surface which attracts oppositely charged ions and water molecules, holding them at the electrode-electrolyte interface by electrostatic forces. Thus, the so called electric double layer is formed. During deposition, ions reach the electrode surface, move to a stable position on it while simultaneously releasing their ligands, release their charges and undergo the stipulated electrochemical reaction. Fresh ions are supplied to the ion depleted region near the electrode by either of the following means: (1) diffusion due to concentration gradient, (2) migration due to the applied electric field and (3) convection currents in the electrolyte. [6, 7, 15]

Electrodeposition is carried out in a three electrode electrochemical cell that contains a “working electrode” a “reference electrode” and a “counter electrode”. For electrodeposition to occur the working electrode must be conducting.

A more practical equation is shown below where the total cathodic charge used in the deposition "Q" (coulomb) is the product of the number of gram moles of the metal deposited "m", the number of electrons taking part in the reduction "n", Avogadro's number "N_A" (the number of atoms in a mole), and the electrical charge per electron "Q_e" (coulomb). To reduce one mole of a given metal "n" moles of electrons are therefore required.

$$Q = m\ n\ N_a\ Q_e \qquad (2)$$

The product of the last two terms in the equation above is the Faraday constant, F. Therefore, the number of moles of metal reduced by charge "Q" can be obtained as:

$$m = \frac{Q}{(nF)} \qquad (3)$$

The total charge used in the deposition can be obtained as the product of the current "I"

$$Q = \int Idt \qquad (4)$$

And so the number of moles deposited can be calculated as:

$$m = \frac{1}{nF}\int Idt \qquad (5)$$

The weight of the deposit "w" (gram) can now be obtained by multiplying the equation above by the atomic weight "M_w" of the deposited metal. To calculate the thickness of the deposit, we have to use the density of the metal "D" (gram/cm^3) where "V" is the volume of the deposited metal in cm^3, "A" is the area of the deposit in cm^2, and "T" is its thickness in cm.

$$D = \frac{W}{V} = \frac{W}{(AT)} \qquad (6)$$

Solving for the thickness we arrive at the following equation.

$$T = \frac{W}{AD} = \frac{M_w}{nFAD}\int Idt \qquad (7)$$

The figure below shows a schematic of an electrolytic cell for the electrodeposition of metal.

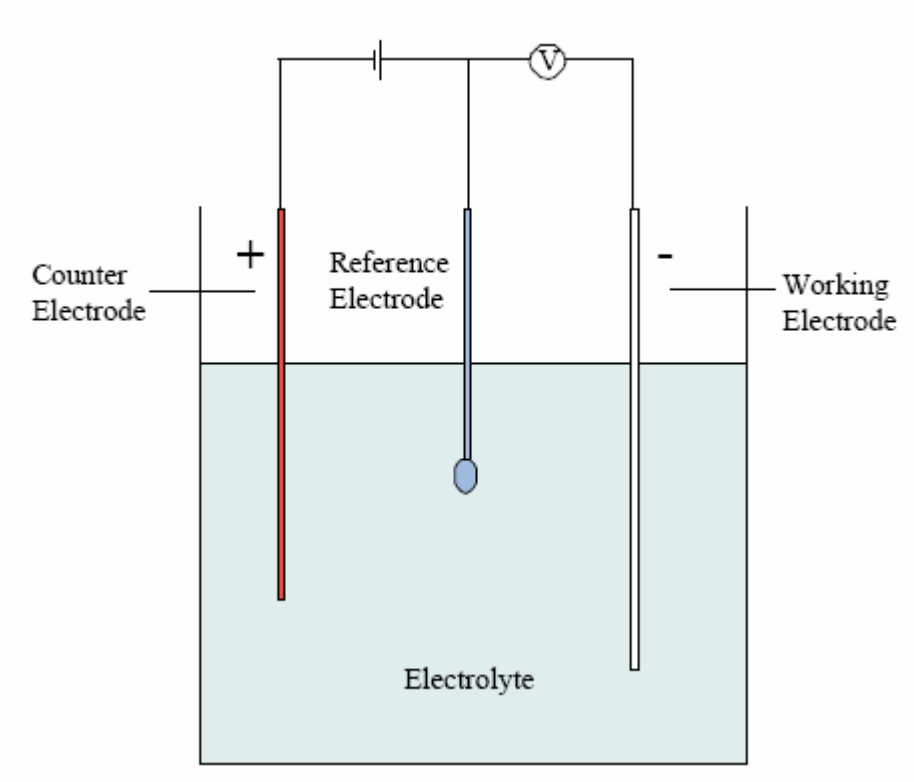

Fig-1.1: Electrochemical cell [13]

1.4.2. Advantages of electrodeposition process

- Selectivity and specificity (from the choice of electrode and potential)
- High sensitivity and low detection limit
- Ready to use compact instruments
- Capability in a single step process to produce metals, alloys and metal-matrix composites in various forms
- Speed and accuracy
- Ability to produce fully dense nanostrtures free of extraneous porosity
- Relatively low cost of application

1.5. Theory of Nucleation and Growth

Nucleation is one of the two major mechanisms of the first order phase transition, the process of generating a new phase from an old phase whose free energy has become higher than that of the emerging new phase. Nucleation occurs via the formation of small embryos of the new phase inside the large volume of the old phase. Another prominent feature of nucleation is metastability of the old phase, i.e., the transformation requires passage over a free energy barrier. This is easily understood by considering the free energy changes associated with the formation of the nucleus. The statement that the free energy per molecule of the new phase is less than that of the solvated phase only applies to the bulk of the new phase. Because the surface molecules are less well bound to their neighbors than are those in the bulk, their contribution to the free energy of the new phase is greater. The difference between the free energy per molecule of the bulk and that of the surface is referred to as the interfacial free energy. (It is sometimes called the surface free energy). The interfacial free energy is always a positive term and acts to destabilize the nucleus. As a consequence, at very small size when many of the molecules reside at the surface, the nucleus is unstable. Adding even one more molecules just increases the free energy of the system. On average, such a nucleus will dissolve rather than grow. But once the nucleus gets large enough, the drop in free energy associated with formation of the bulk phase becomes sufficiently high that the surface free energy is unimportant, and every addition of a molecule to the lattice lowers the free energy of the system. There is an intermediate size at which the free energy of the system is decreased whether the nucleus grows or dissolves, and this is known as the critical size. This phenomenon is referred to as the Gibbs-Thomson effect. If the supersaturation is high enough, the critical size can be reduced to less than one growth unit. Then the barrier vanishes and the old phase becomes unstable so that an infinitesimal fluctuation of an order parameter, such as density, can lead to the appearance of the new phase. The rate of generation and growth of the new phase is then only limited by the rate of transport of mass or energy. This second process is referred to as spinodal decomposition, and the boundary between the regions of metastability and instability of the old phase is called a spinodal line (Binder and Fratzl 2001; Kashchiev 2003). The existence of a critical size has a number of implications. First and foremost, because nucleation of the new phase is the result of fluctuations that bring together sufficient numbers of molecules to exceed the

critical size, the probability of nucleation will be strongly affected by the value of the critical size. This means that nucleation can be controlled, to some extent, by modulating the critical size, which is in turn a function of the interfacial energy. The smaller the interfacial energy, the smaller the critical size and the more likely nucleation becomes for any given supersaturation. As a consequence, by varying either the solution composition or the supersaturation, the probability of nucleation can be manipulated [16].

Consider a spherical nucleus of radius r, as illustrated in Figure, nucleating within the bulk solution. (This is referred to as homogeneous nucleation.) The free energy change per molecule (Δg) is given by the sum of bulk (Δ_{gb}) and surface terms (Δ_{gs}), namely:

$$\Delta g = \Delta g_b + \Delta g_s$$

$$= -\left[\frac{4/3\,\pi r^3}{\Omega}\right]\Delta\mu + 4\pi r^2\alpha \qquad (8)$$

where Ω is the volume per molecule, and α is the interfacial free energy. The first term is negative and varies as the cube of r, while the second term is positive and varying as r^2.As shown in Figure 6b, the sum of the two terms has a maximum that occurs when $d\Delta g/dr = 0$. The value of r at this point can be found by taking the derivative and setting it equal to zero.

This is known as the critical radius, r_c, and is given by:

$$r_c = \frac{2\Omega\alpha}{\Delta\mu}$$

$$= \frac{2\Omega\alpha}{KT\sigma} \qquad (9)$$

The same analysis can be performed for heterogeneous nucleation, i.e., nucleation at a foreign surface. There are now two interfacial energies to consider, one between the crystal and solution and the other between the crystal and the substrate, as illustrated in Figure. If we assume, for simplicity, that the nucleus is a hemisphere of radius r, we have:

$$\Delta g = -\left\{[(2/3)\pi r^3]/\Omega\right\}\Delta\mu + \pi r^2(2\alpha_{lc} + \alpha_{sc} - \alpha_{ls} \qquad (10)$$

Where the subscripts “sc”, “lc”, and “ls” refer to substrate-crystal, liquid-crystal, and Liquid-substrate respectively. The new expression for r_c becomes:

$$r_c = 2\Omega\alpha^{/} \Big/ K_B T\sigma \qquad (11)$$

$$\alpha^{/} = \alpha_{lc}\left\{1-(\alpha_{ls}-\alpha_{sc}) \Big/ 2\alpha_{lc}\right\}$$

The term in the brackets is always less than one, provided the free energy of the crystal substrate interface is less than that of the substrate-liquid interface. Thus the value of r_c at the substrate is reduced below that for nucleation in free solution [17].

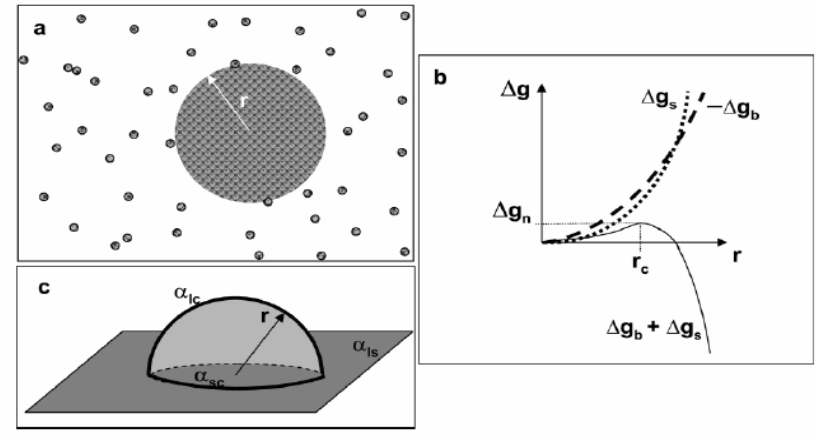

Fig – 1.2(a) Formation of a spherical nucleus of radius *r* from a solution leads to the free energy changes shown in (b). The cross-over of the bulk and surface terms combined with their opposing signs leads to a free energy barrier. (c) Heterogeneous formation of a hemispherical nucleus at a foreign substrate.

The increase in the size of the particle beyond the critical size is called growth. Like nucleation, growth is dependent on the thermal fluctuations.The growth rate is zero at the equilibrium temperature T_0, as well as at 0K.It passes through a maximum at some intermediate temperature, which turns out to be higher than that for the nucleation maximum as shown in fig1.3.

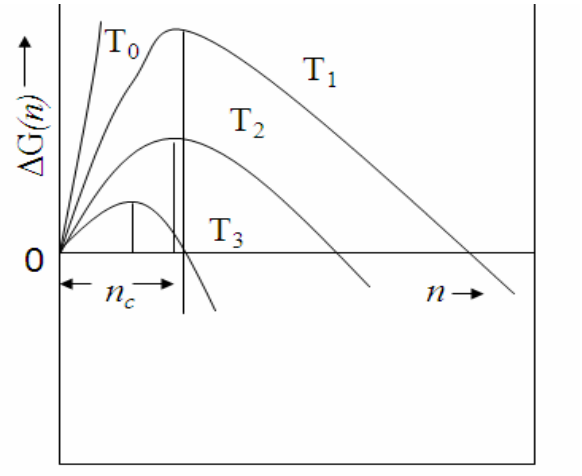

Fig-1.3. The free energy of nucleation as a function of radius r of a spherical nucleating particle.

The grain size of the product phase depends on the relative rates of nucleation and growth. Each nucleating particle becomes a grain in the final product. So a high nucleation rate means a large number of grains. When this is combined with low growth rate, more time is available for further nucleation to take place in the parent phase that lies between slowly growing particles. So the combination of high nucleation rate and a low growth rate yields a fine grain size which is show in fig 1.3.

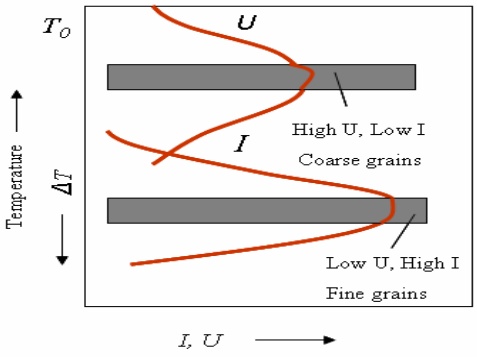

Fig-1.4: The Nucleation rate I and the growth rate U as a function of temperature

In fig 1.4, the temperature of maximum rate of nucleation is lower than the temperature of maximum growth rate. An increase in cooling rate lowers the effective transformation temperature and results in the combination of high nucleation rate and a relatively slow growth rate and therefore yields a fine grain size [18, 19].

1.5.1. Nucleation and growth stages of metal films

Nucleation and growth are one of the two major mechanisms for the formation of thin films during electrodeposition. The formation mechanism of pure metal films by electrodeposition is illustrated in Figure 1.5 (Gerischer, 1960).

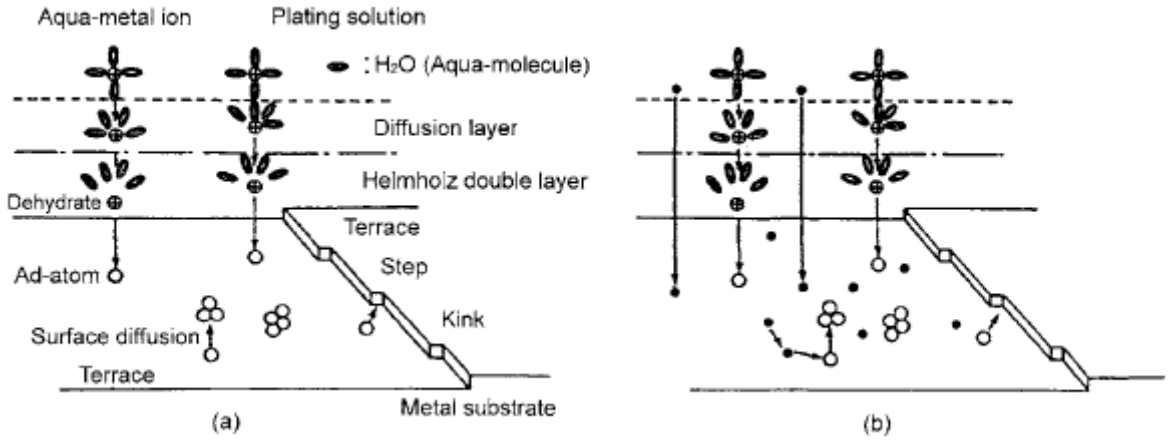

Fig-1.5: The initial stages of electrocystallization for (a) pure metals and (b) alloys

Metal ions, which are generally hydrated or complexed in a bulk electrolyte, first diffuse toward a cathode (substrate) through the potential gradient. After these ions pass through a diffusion layer and an electrical double layer (Helmholtz layer) present on top of the cathode surface, they will be stripped from the hydrate or complex ions, and become bare metal ions. The bare metal ions are then discharged by combining with electrons on the cathode, and become neutral atoms (adatoms). The adatoms now start migrating over the substrate surface until they are adsorbed at active sites, finally forming a strong chemical bond with the substrate. Kinks or steps present on the substrate surface are believed to be active sites for adatoms to be finally adsorbed. It can be seen that the successive adsorptions of adatoms at such sites result in the continuous spreading of the mono-atomic layer over the substrate surface [20].

The theory of metal deposition is based generally on the Butler-Volmer [21] equation giving the current density on a metal substrate as function of overvoltage η.

$$i = i_0\left[\exp\left(\frac{\alpha zF\eta}{RT} - \frac{(1-\alpha)zF\eta}{RT}\right)\right] = i_0 V(\eta) \qquad (12)$$

This equation is derived under the assumption that the rate determining process is the charge transfer reaction. A second tacitly made assumption is that the surface is homogeneous so that the current density is uniformly distributed over the entire solid surface. Recognizing that metal deposition is a crystal growth process. Volmer and Weber [22] suggested that the overpotential must depend on the formation kinetics of 3D or 2D crystalline clusters as required by the Gibbs crystal growth theory [21]. According to the prevailing mechanism the current can be either proportional to the exponent of the reciprocal of overpotential-1/ η or to that of the reciprocal of the squared overpotential, -1/ η^2 for the 2 or 3D case, respectively. These relations expected to be valid under steady state conditions have not been convincingly verified but 2 and 3D nucleation has been demonstrated to play a significant role in metal deposition studying the morphology of deposits [23]. Nucleation is a very important process in metal deposition. On one hand, the competition between growth and nucleation determines the granularity of the deposit. The higher the nucleation rate during deposition, the finer are the crystal grains of the deposit. On the other hand, the forms of the growing crystals determine the general appearance and structure of the deposit. With a higher growth rate of the crystal grains normal to the substrate surface, for instance, a fibrous structure of the deposit is obtained. Or, with large developed crystal faces parallel to the substrate a brightening effect can be achieved. The formation of a new phase, as required in the initial stages of metal deposition on a foreign substrate, is kinetically limited by the specificity of the Gibbs formation energy dependence of a cluster of the new phase on its size *N*, *N* being the number of atoms forming the cluster. The Gibbs formation energy, Δ*G* (*N*), of a cluster of *N* atoms contains two terms.

$$\Delta G\ (N) = -\mathrm{N}ze\eta + \Phi\ (\mathrm{N}) \qquad (13)$$

The first term is connected with the transfer of *N* ions from the ambient phase (the electrolyte) to the substrate surface under the action of the overvoltage $|\eta|$.

This term is always negative. The second term, Φ (*N*), represents an excess free energy taking into account energy contributions derived from the deviation of the new phase from the bulk phase. Along with the creation of new boundaries additional effects, e.g. internal

strains, deviation from the bulk atom arrangement, etc. can also affect this term. The relation $\Delta G\ (N) - N$ is a function with a maximum determining an energy barrier ΔGcrit (N) at a cluster size Ncrit, known as the nucleus. The existence of an energy barrier makes the nucleation a probability process, with a rate J (nuclei/cm^{2}s^1) given by the probability for their formation:

$$J=A_J \exp(-\Delta G_{crit}/KT) \qquad (14)$$

Where A_J is a constant of proportionality. The energy (fluctuation) barrier ΔG_{crit} can be found as the maximum of the $\Delta G\ (N)$ function, [17].

The initial stages of thin film growth have been categorized in to three growth modes. These modes include: (a) Volmer-Weber (V-W), (b) Frank-van der Merwe (F-M), and (c) Stranski-Krastanov (S-K) type.

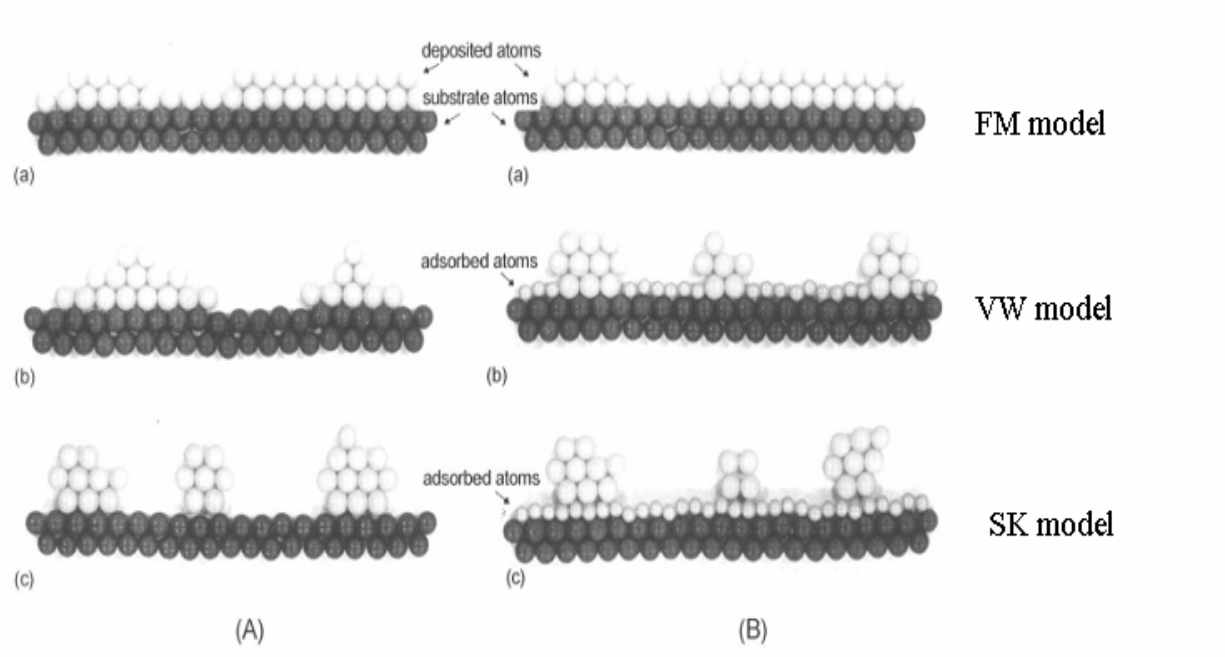

Fig-1.6: Three modes for describing the initial stages of thin-film growth, (a) Volmer-Weber (V-W), (b) Frank-van der Merwe (F-M), and (c) Stranski-Krastanov (S-K) types.

The three modes of atom deposition and film formation on ideal surface id shown in fig.1.6 [20].

The general picture of the step by step growth process emerging out of various experimental and theoretical studies can be presented as follows: [7]

1. The unit species, on impinging the substrate, lose their velocity component normal to the substrate and are physically absorbed on the substrate surface.
2. The adsorbed species are not in thermal equilibrium with the substrate initially and move more over to the substrate surface .In this process they interact themselves , forming bigger clusters.
3. The clusters or the nuclei, as they are called, are thermodynamically unstable and tend to desorbs in a time depending on the deposition parameter. If the deposition parameters are such that a cluster collides with other adsorbed species before getting desorbed, it starts growing in size. After a certain critical size is reached, the cluster becomes thermodynamically stable and the nucleation barrier is said to have been overcome.
4. The critical nuclei grow in number as well as in size until a saturation nucleation density is reached. The nucleation density and the average nucleus size depend on a number of parameters such as the energy of the impinging species, the rate of impingement , the activation energy of the adsorption, desorption and thermal diffusion and the temperature, topography and the chemical nature of the substrate. A nucleus can grow both parallel to the substrate by surface diffusion of the adsorbed species. The grown nuclei are called islands.
5. The next stage in the process of formation is the coalescence stage, in which the small islands start coalescing wit each other in an attempt to reduce the surface area. This tendency to form bigger islands is termed agglomeration and is enhanced by increasing the surface mobility of the adsorbed species.
6. Larger islands grow together, leaving channels and holes of uncovered substrate .The structure of the films at this stage changes from discontinuous island type to porous network type. A completely continuous film is formed by filling of the channels and holes.

1.6. Factors affecting on nucleation and growth of phases during electrodeposition of thin film

The nucleation and growth of the deposits is determined by a number of parameters such as current density, bath composition, and temperature, electrode shape, nature of the counter electrode and the mechanical agitation of the electrolyte.

1.6.1. Temperature

The velocity (diffusion and migration) of metal ions and inhabitor molecules are the function of temperature ($D=D_0e^{-Q/RT}$). A high temperature causes an increased in ion supply towards the cathode and the cathodic overpotential decreases. This increases the energy of the nucleation. An increased energy for the nucleation process means decreased rate of nuclei formation and preferred growth of existing nuclei. The consequences are the formation of coarse grains. Activation energy for the nucleation A_k is related to cathodic overpotential Δ_g i.e,A_k is proportional to $1/\Delta_g$ [24] .The viscosity of electrolyte decreases at high temperature. The adsorption rate of inhibitor molecules decreases at high temperature and increases the surface energy of the crystallites. Volmer has shown that A_k is proportional to 3rd power of the surface energy ($A_K \propto \sigma^3$) [22]. Due to high desorption of inhibitors at high temperature σ was increased resulting in an increased grain growth.

According to thermodynamics the addition of complex formers (additives) generates more or less stable complexes. The increased dissociation of a complex at high temperature is the region for an increased metal ion concentration. Increased concentration means decreased cathodic overpotential.This results formation of large grains [24,25,26,27,28].

The SEM micrograph shows that the film deposited at room temperature comprised of uniformly size grain which are closely packed together. The substrate was well covered with the deposit without any cracks.

This figure shows that if we increase the temperature of the bath then cystal size increases, but if we decrease the temperature of the bath the crystal size decreases from micro range to nanorange, because low temperature may avoid undesirable interdiffusion between adjacent layers and structures and allows uniform modification of surfaces and structures with reduced grain size [26]

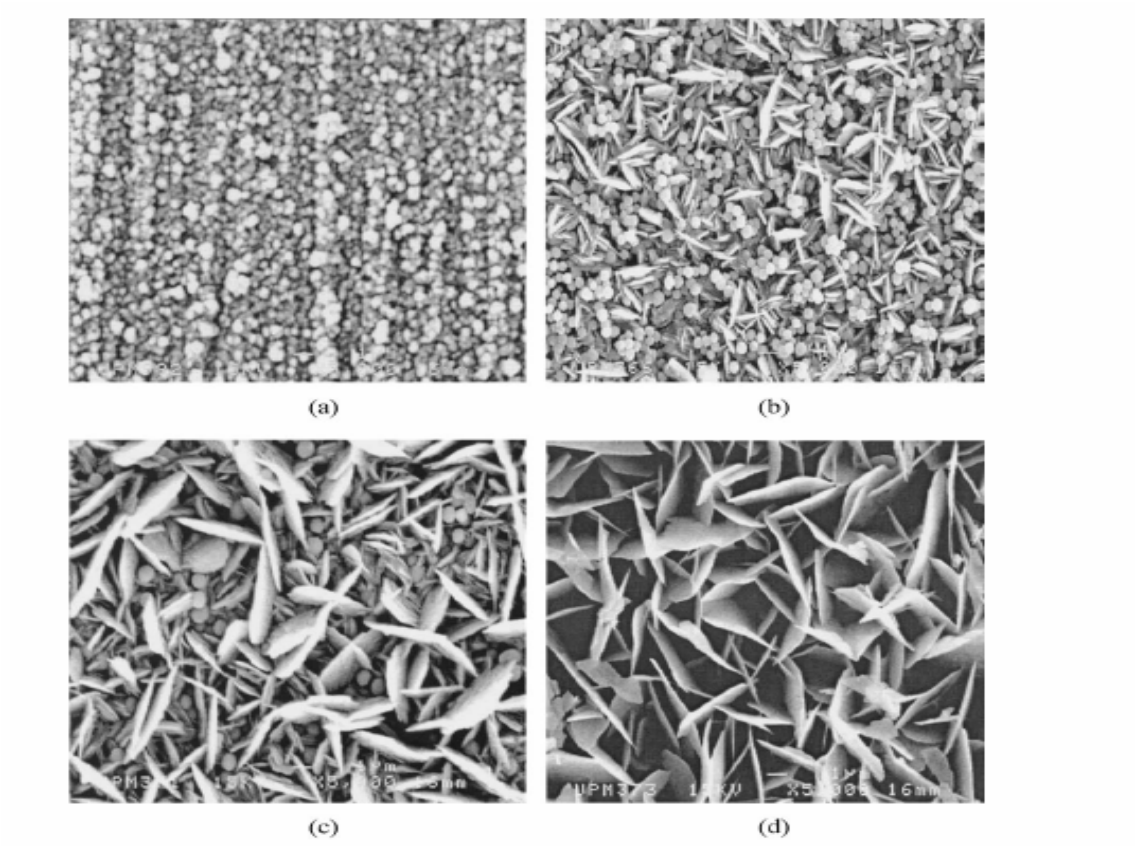

Fig-1.7: SEM micrograph of Cu_2SnSe_4films prepared at different bath temperatures (a) 28, (b) 35, (c) 45 and (d) 55 ^{0}C.

Increase in temperature usually decreases polarization, increases concentration of metal in the cathode diffusion layer and may affect the cathode current efficiency of deposition of metals, particularly those deposited from complex ions.

A series of electrodeposition runs was performed at different temperatures ranging from 25˚C to 70˚C. The variation of cathode current efficiency with temperature is demonstrated in Fig.1.9. The deposit obtained at 45˚C was found to have the best physical characteristics such as appearance and hardness.

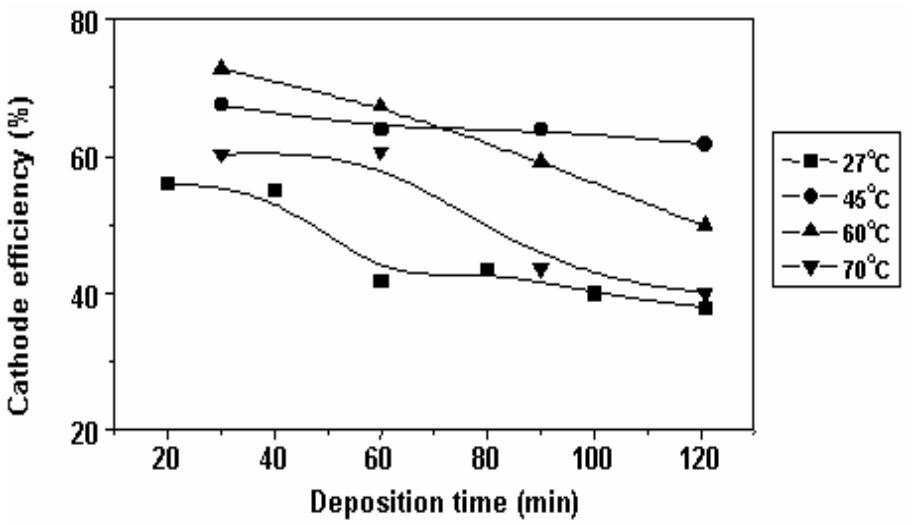

Fig-1.8: Effect of bath temperature on cathode current efficiency

Figure presents stress-strain curves for two different grain sizes tested at room and low temperatures. Decreasing test temperature increased the strength significantly.

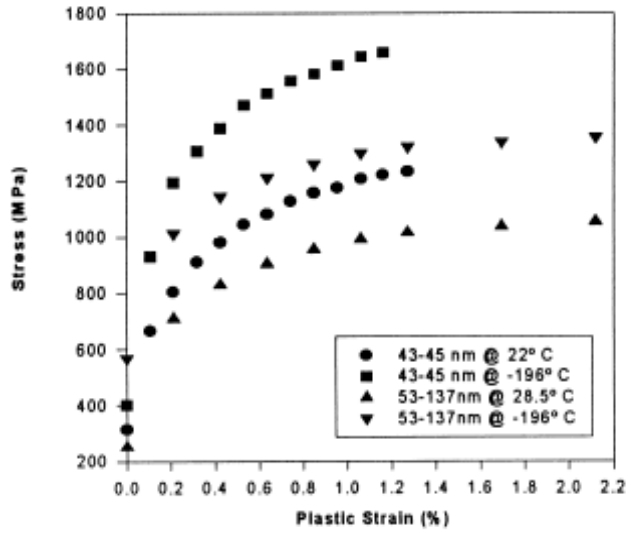

Fig-1.9: Effect of grain size on tensile stress-strain curves of nickel at RT and low temperature.

1.6.2. PH or Acid Concentration

As the PH of the electrolyte increased the current efficiency, grain size and stresses in the deposit increased. It is related to decrease of hydrogen evolution reaction and hydrogen absorption. When the PH of the electrolyte increased open circuit potential moved to a

negative potential and the limiting current density for the metal reduction slightly increased indicating that polarization had decreased. The open circuit potential of the metal does not change with time, its value depends on the solution PH and it becames more negative as PH decreases. Decreasing the PH of electrolyte led to the increase of hydrogen evolution reaction and hydrogen bubbles which cling to the surface and decreases the effective area of the metal reduction reaction and this hydrogen evolution increases the coefficient of mass transfer and the deposits is in the powder or dendritic form [27]. Decreasing the PH of the solution increases the current density due to an increase in the H^+ ion. This increase in H^+ ion enhances the reduction potential. In this condition large deposition current exists and hydrogen gas evolved, leading to irregular surface of the film[29,30].A higher hydrogen overvoltage by lower hydrogen concentration of the electrolyte resulted in the decrease of the hydrogen evolution reaction and hydrogen bubbles leading to a decrease of occupied area by hydrogen reaction, which caused a decrease in all the resistance of the impedance spectra with PH.Due to decrease of hydrogen evolution mass transfer is controlled and compact deposits are obtained. Liquid gas phase by hydrogen gas act as an obstacle for the ion conductivity of the electrolyte. Hence higher PH of the electrolyte increases the solution conductivity and the adsorption of intermediate phases and decreased the activation polarization for the metal deposition and so encourage the formation of dense compact deposits. Higher Ph of the solution also decreases the activation and diffusion polarization, decreasing the total over potential for the metal electrodeposition.This higher PH increases the grain size of the deposits by reducing the nucleation rate. Residual tensile stresses of the deposits increased with the PH value [24, 27, 30].

Table-1: Variation of residual stresses with PH value

PH value	Temperature in ^{0}c	Residual Stresses in (Mpa)
1	60	5.9
2	60	6.3
3.5	60	29.7

The XRD results of the Ni-Fe deposits obtained from various PHs and temperatures; (a) pH 1, (b) pH 2 and (c) pH 3.5 at 60 ^{0}C, and (d) pH 2 at 50 ^{0}C, and (e) pH 2 at 70 ^{0}C. Lower pH decreased the peak intensity and broadened the peak. This suggests that the crystallinity and grain size in the deposits decreased with the decrease of bulk PHs due to a high polarization.

According to the classical theories on electrochemical phase formation and growth, the three dimensional (3D) nucleation rates, J is given by

$$J = K_1 Exp\left[-4BV_m^2\sigma^3 \Big/ 27(ze\eta^2 KT) \right] \qquad (15)$$

where $k_{=1}$ is the rate constant; B the geometric factor depending on the geometry; Vm is the area occupied by one atom; σ the average specific surface energy; z the electronic charge of the ion; e the charge of the electron; k the Boltzmann constant; and η the overpotential. As shown in the electrochemical behavior, a higher pH decreased the activation and diffusion polarization, decreasing the total over potential (η) for the alloy electrodeposition. Therefore, a higher pH increased the grain size of the deposit by reducing the nucleation rate, J[31].

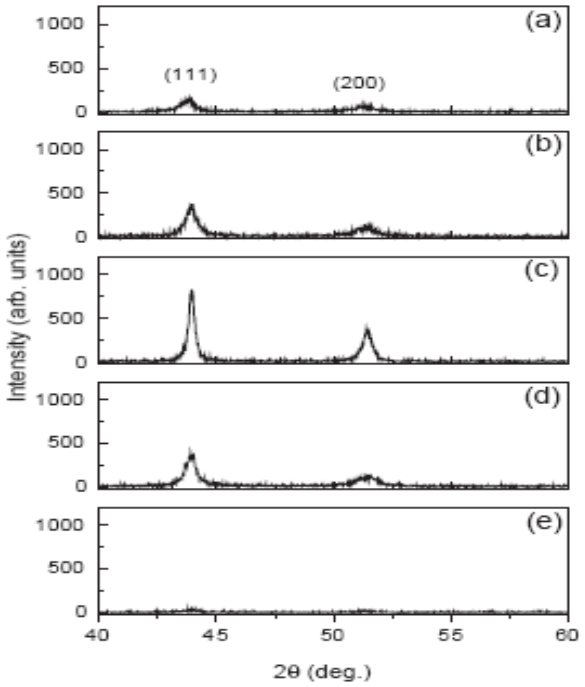

Fig-1.10: XRD results on the deposits obtained from different PH and temperature; (a) pH 1, (b) pH 2 and (c) pH 3.5 at 60 ^{0}C, and (d) pH 2 at 50 ^{0}C, and (e) pH 2 at 70 ^{0}C.

The effect of pH on microstructural and mechanical properties of electrodeposited nickel produced in this study. In the absence of continuous nucleation of new grains, the deposits consists of columnar grains, whose size becomes larger with thickness . The disc deposited at pH 5 2.8 showed columnar grains and its average crystallite size increased from 283 nm on the substrate side (sub) to 342 nm on the solution side (sol). As pH was increased, the crystallite size decreased and became more uniform through the thickness. The smaller crystallite size on the solution side suggests that increasing the pH enhanced the nucleation rate of nickel crystals. When pH was raised above 4.8, the average crystallite size started increasing again. As the results for pH 5 5.1 demonstrate, the increase in crystallite size was more pronounced on the substrate size. This observation suggests that in this disc the decrease in pH during deposition brought the pH level back up to the optimum range, where nucleation is enhanced. Consistent with this hypothesis, an increase in the deposit thickness at a high pH level resulted in a finer crystallite size measured on the solution side [26].

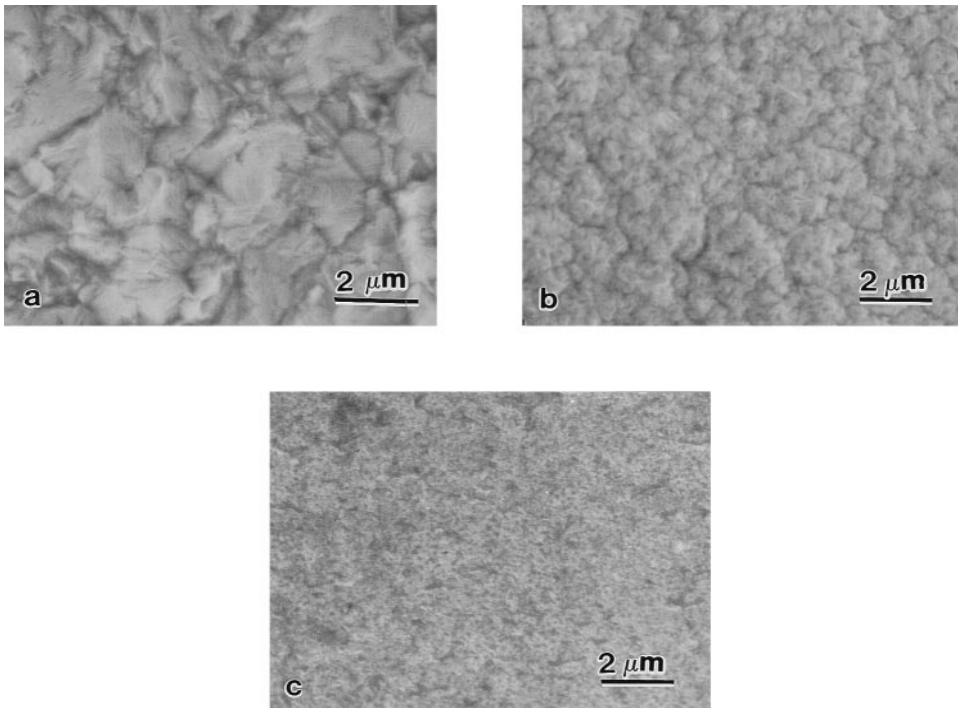

Fig-1.11: SEM micrographs from the surface of discs deposited at (a) pH=5 2.8, (b) pH= 4.1, and (c) pH= 4.67.

The decrease in crystallite size achieved by raising the electrolyte pH resulted in significant increases in strength and strain hardening.

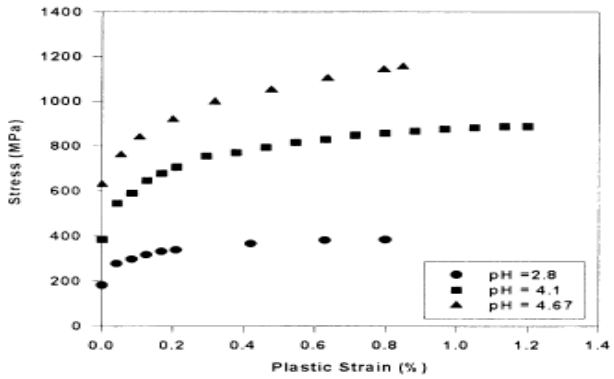

Fig-1.12: Tensile stress-strain curves for specimens fabricated at three different pH levels.

1.6.3. Current Density

At low current densities the discharge of ions occurs slowly, and so the rate of the growth of the nuclei should exceed the rate at which new ones form; the deposits obtained under these conditions should be coarsely crystalline. As the current density is raised the rate of formation of nuclei will be greater and the deposit will become finer-grained. At very high currents the solution in the vicinity of the cathode will be depleted in the ions required for discharge, and, as a result, the crystals will tend to grow outward regions of higher concentration; the deposit then consists of "trees," nodules or protruding crystals. If the current density exceeds the limiting value for the given electrolyte, hydrogen will be evolved at the same time as the metal is deposited; bubble formation often interferes with crystal growth, and porous and spongy deposits may be obtained. The discharge of hydrogen ions frequently causes the solution in the vicinity of the cathode to become alkaline, with the consequent precipitation of hydrous oxides or basic salts; if these are included in the deposit, the latter will be fine-grained and dark in appearance.

Surface morphologies of the Zn films deposited by potentiostatic methods are examined using an SEM. The images are given in. The surfaces of the films appear to be smooth and densely covered. The crystallites, however, get finer when deposited at higher cathodic potential or current density [32, 33].

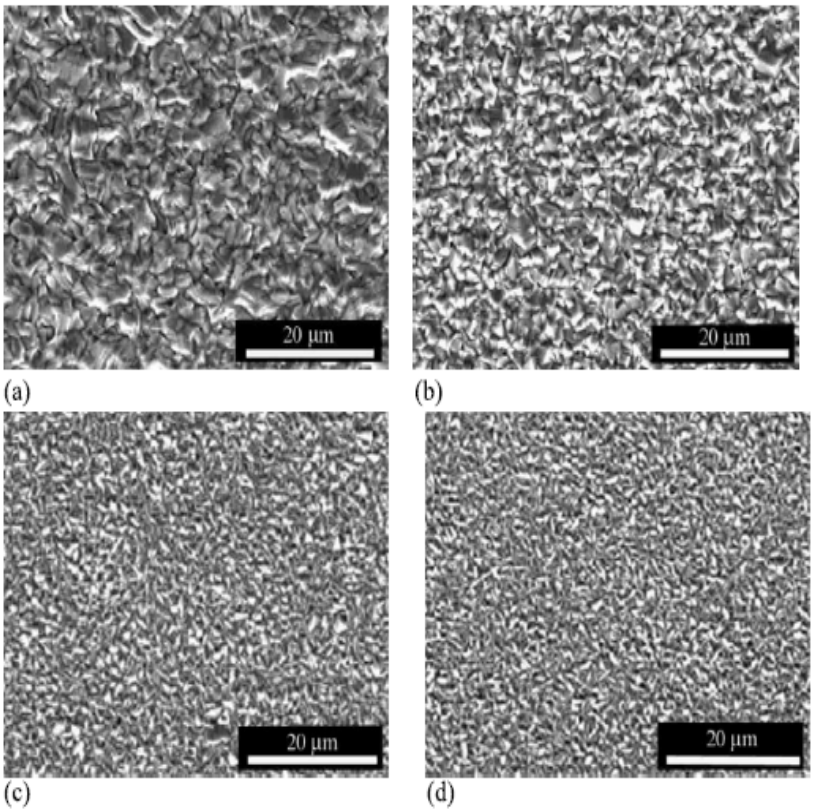

Fig-1.13: SEM images for zinc electrodeposited at different current densities. (a) 0.4 A cm^{-2}, (b) 0.8 A cm^{-2}, (c) 1.2 A cm^{-2}, (d) 1.6A cm^{-2}.

1.6.4. Metal ion concentration

The effect of concentration of metal ion on nuclei size distribution and governing mechanisms is given in Fig. 10a and b, for lower and higher metal ion concentrations, respectively. Stage I represents the initial conditions prior to the onset of the reduction reaction. A liquid boundary film layer adjacent to the solid substrate and a solution bulk are depicted. The liquid boundary film is presented in the simplest possible terms, as used by Scharifker- Hills [34], thus no double layer properties were considered. At the very beginning of electro reduction the number of metal atoms produced on the surface is a function of initial bulk concentration. In the case of lower metal concentration, Fig. 1.15(a) the metal atoms are spaced further apart compared with the case with higher metal concentration, Fig. 1.15(b). Once distributed over the surface in the atomic state, atoms must travel toward each other in order to minimize the surface energy. Atoms spaced further apart have to travel longer distances in order to group together and form a nucleus. Since this is energetically unfavorable they have to group together with the nearest neighbors, resulting in

large number of small nuclei. On the other hand, when the initial number of reduced metal atoms is large, the close proximity of atoms will result in grouping to form a large nucleus. The size of each nucleus determines the size of its diffusion zone. Decrease of nuclei population density with the increase of concentration was also predicted by the Scharifker-Hills model [12]. According to the model, nuclei population density can be calculated for different copper concentrations as a function of peak current i_{max} and corresponding peak time, t_{max}.

$$N_0 = 0.065\left(\frac{1}{8}\pi C_0 V_m\right)^{1/2}\left(\frac{nFC_0}{i_{\max} t_{\max}}\right)^2$$

where, n, number of electrons involved; F, Faraday constant; C_0, concentration of species in the bulk; V_m, molar volume; t_{max}, peak time and i_{max}, peak current density[35].

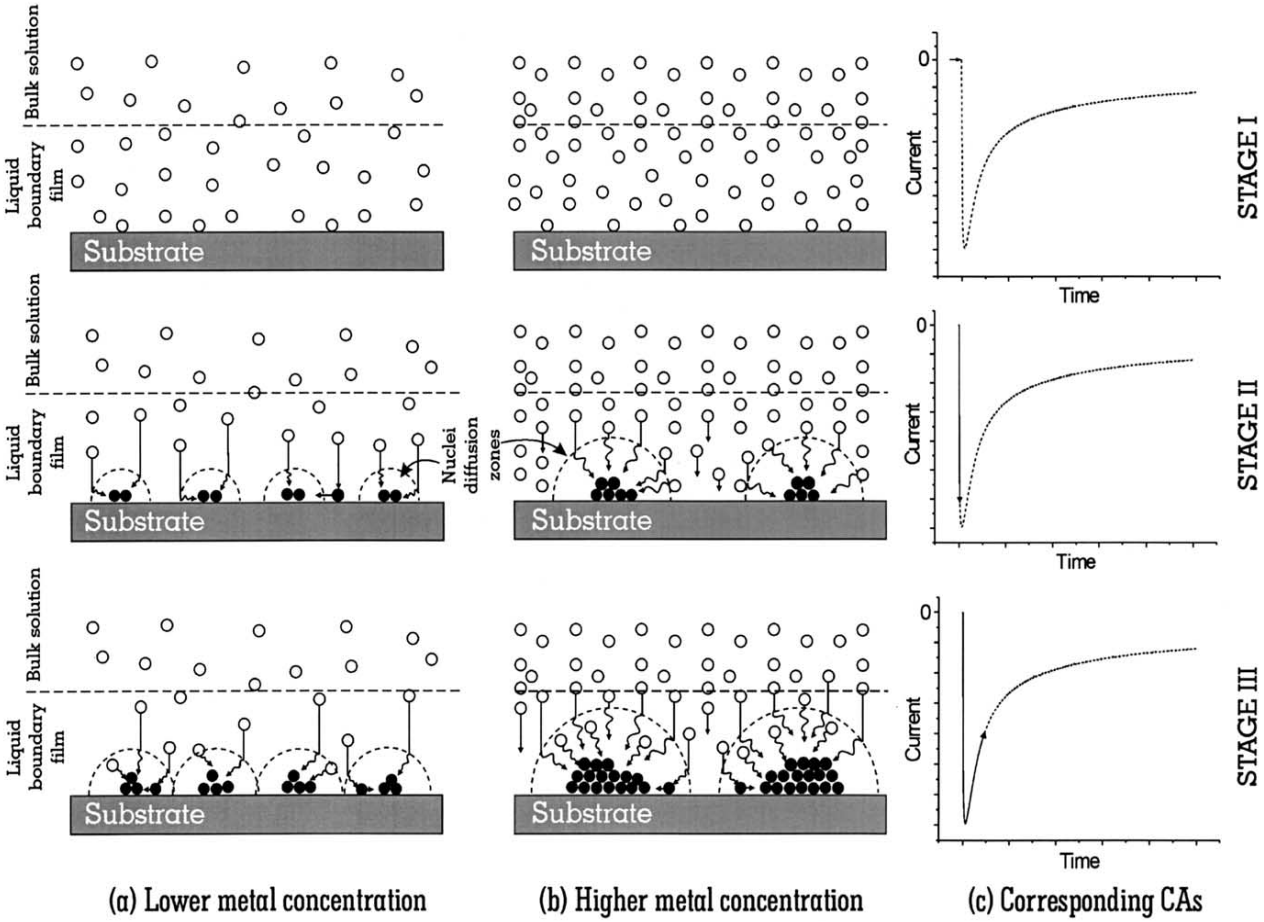

Fig-1.14: Schematic presentation of phenomena involved during nucleation at various stages of chronoamperometric experiment for (a) lower and (b) higher concentration of metal ions. Depicted stages are (I) prior to electroreduction, (II) state at the onset of reduction and (III) steady state of electroreduction.[35]

The effect of copper concentration on the morphology of copper nuclei was studied at pH 1, 2, and 3. Fig. 1.16(a- c) represents the results from the copper deposition study at pH 1 in 0.01, 0.025 and 0.05 M Cu^{2+} solutions.

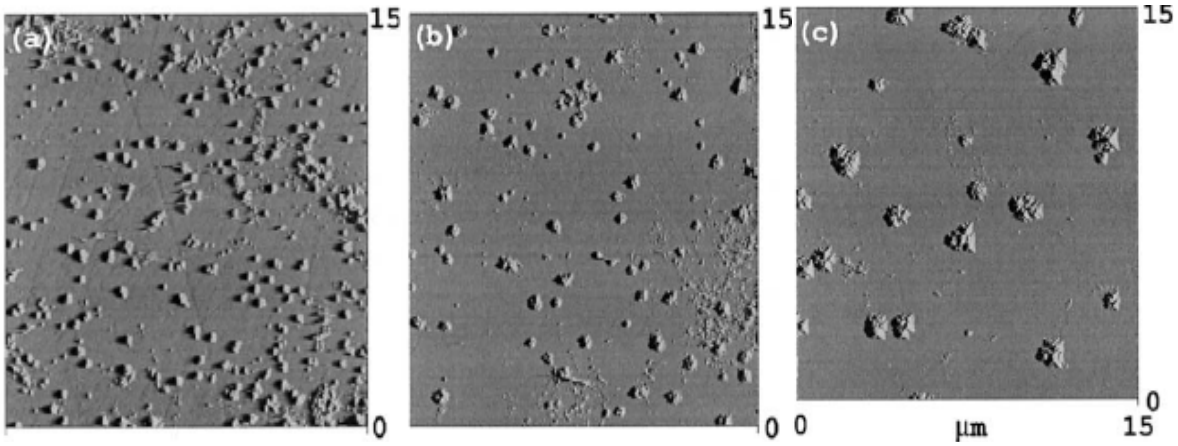

Fig-1.15: Effect of concentration on the morphology (AFM) of copper deposited under potentiostatic conditions at-450 mV for 0.8 s. Copper concentrations (a) 0.01 M, (b) 0.025 M, (c) 0.05 M. All solutions at pH 1 [35].

For the 0.01 M copper concentration, Fig. 1.15 (a), the nuclei were relatively small and densely distributed on the surface. At a higher copper concentration, Fig. 1.15(b), the size of nuclei increased, but the nuclei population density decreased, which was even more pronounced at a higher copper concentration, Fig. 1.15(c).

The effects of the electrolyte concentration and of current density are to a great extent complementary by increasing the concentration or by agitating the solution, higher current densities can be used before coarse deposits are formed, or before hydrogen evolution occurs with its accompanying spongy or dark deposits. The influence of concentration on the rate of nucleus formation is uncertain; since increase of concentration tends to give firm, adherent deposits, some workers have expressed the opinion that the presence of the large number of ions in a concentrated solution favors the formation of fresh nuclei. Certain experiments, however, indicate that the rate of formation of nuclei is actually decreased by increasing concentration, but the improvement in the deposit is due to an increase in the rate of growth of crystals over the cathode surface, combined with a decrease in the rate of growth in a perpendicular direction [36].

The TEM micrographs of silver nanoparticle prepared by sonoelectrodeposition are shown. This figure shows that with the increase of concentration of electrolyte, the formation of nuclei decreased but the growth rate is increased. With low concentration of silver nitrate solution (*e.g.* 0.0118 mol·L−1) the spherical nanoparticles were prepared **(a)**. Silver nanoparticles were aggregation when the AgNO3 concentration was 0.0236 mol·L−1**(b)**. With the AgNO3 concentration further increasing to 0.0472 mol·L−1, silver particles grew into dendrites (**c)**. It might be that the excess of silver in the solution favored the aggregation and grew into the dendritic structure of silver clusters [37].

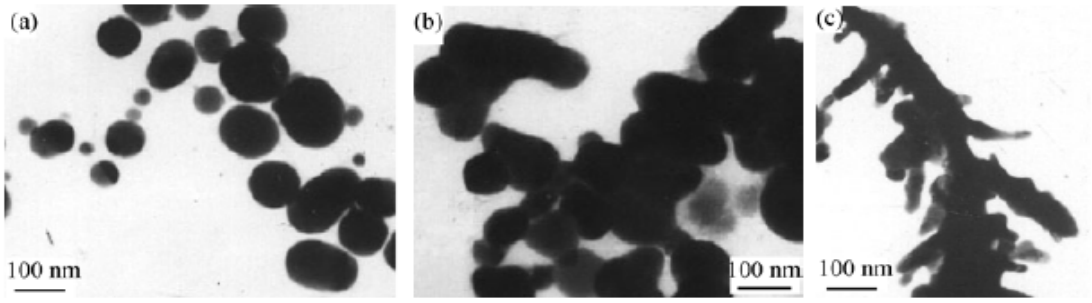

Fig-1.16: TEM micrographs of silver nanoparticles at different concentrations of AgNO3: (a) 0.0118 mol·L−1; (b) 0.0236 mol·L−1; (c) 0.0472 mol·L−1

1.7. Sonoelectrochemistry

Sonoelectrochemistry is the study of the effects of the combination of ultrasonic radiation with electrode processes occurring at surfaces of electrodes immersed in a solution in an electrochemical cell. Ultrasound introduces energy into the system, both in homogeneous solution and on solid surfaces. Resulting phenomena include cavitations, acoustic microstreaming, mixing, emulsification, and enhanced hydrodynamics. There are also effects on suspended solids, particles, and nucleation enhancing species and on dissolved gases. All of these can influence an electrochemical process. The beneficial effect of sonochemistry with electrochemistry includes acceleration of mass transport, cleaning and degassing of the electrode surface and an increased reaction rate and the particle size can be controlled by adjusting various parameters such as current density, deposition temperature and sonic power.Sonochemistry is the research area in which molecules undergo a chemical reaction due to the application of powerful ultrasound radiation(20kHZ-10MHZ) .T he

physical phenomena responsible for the sonochemical process is the acoustic cavitation.Sonochemistry is the creation, growth and collapse of a bubble that is formed in the liquid. Propagation of ultrasound radiation creates rarefraction and compression within the molecules of the electrolyte and ruptures the chemical bonds results creation of bubbles. The stage leading to the growth of the bubble occurs through the diffusion of solute vapour into the volume of the bubble. The last stage is the collapse of the bubble, which occurs when the bubble size reaches its maximum value. According to the hotspot mechanism when the bubble collapses, chemical bonds are broken and very high temperatures are obtained. This collapse occurs in less than a few nanoseconds, and very high cooling rates in excess of 10^{11} k/s are also obtained.

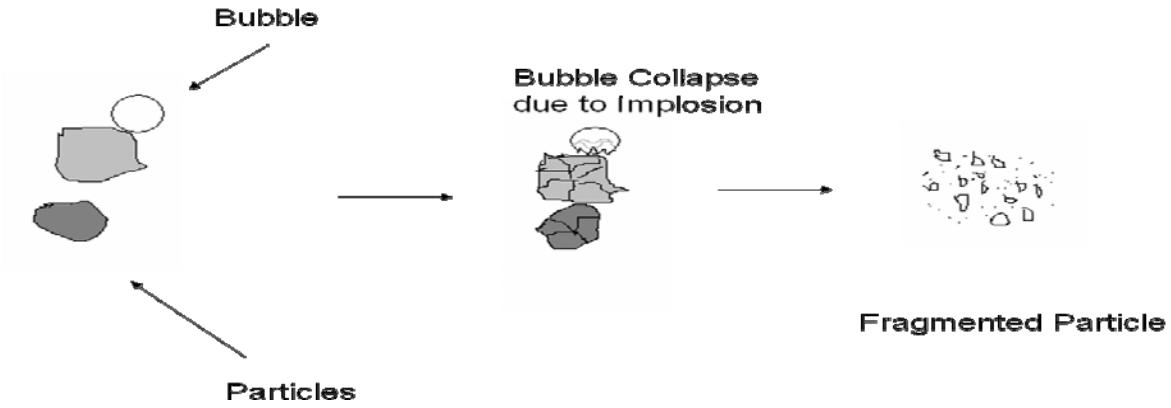

Fig-1.17: Sono- Fragmentation

A number of possible effects of ultrasound upon an electrochemical system may be predicted:

- A general improvement of hydrodynamics and movement of species;
- The alteration of concentration gradients at various points in the reaction profile, and consequent switching of kinetic regimes with effect on mechanism and reaction products;
- A cleaning and abrading effect upon an electrode surface, thus obviating fouling problems, or else altering the nature of coatings that manage to form;
- Sonochemically-induced reactions of intermediate species that have been generated electrochemically;
- The sonochemical formation of species that react electrochemically in conditions

where the silent system is electro inactive.

Sonoelectrodeposition method was mild, convienent, and non pollutionary.It has been becoming an effective approach in the synthesis of nanomaterials [5, 37, 38].

1.8. Effect of ultrasonic agitation on some properties of electrodeposited thin film

The application of ultrasound in electrodeposition is controlling the supersaturation, nucleation and crystal growth during the acid-base reaction crystallization. Ultrasonic irradiation and cavitation in liquid and solid–liquid systems can produce a series of unique chemical and physical effects. These effects enhance reaction rate and product yield, and facilitate mass transfer and reactant diffusion. The proper use of ultrasonics can significantly improve crystal nucleation and growth. Ultrasonic vibration and cavitation in the liquid can play a unique role in mixing reactants uniformly and rapidly. The shock wave and microjet from local high pressure of the cavitation collapse can accelerate the motion of the liquid molecules and increase molecular impacts so as to prompt reaction and nucleation. Because the thickness of the stagnant film and the adsorption layer adjacent to the growing crystal surface depends on the relative solid–liquid velocity, ultrasonically mediated solute transfer will help promote crystal growth in solution. The cavitation collapse may also act as a crystal nucleation center in solution. A recent study has also suggested that the ultrasound produces a thin-film surface layer on the crystal in which the crystallizing molecules can better align themselves for incorporation in the unit cell. Ultrasound can also cause macrostreaming by incident and reflective waves. These ultrasonic effects are believed to be superior to conventional agitation in controlling and prompting reaction rate, level of supersaturation, nucleation and crystal growth.

1.8.1. Effect of ultrasound on the promotion of the reaction and nucleation

After the rapid addition of the reactant, sonication of the reaction is mainly used to quickly distribute the reactant and ensure uniform supersaturation of the solution throughout the vessel. Since the metastable zone is narrowed by sonication, nucleation occurs rapidly at a modest level of supersaturation during the several seconds of sonication. The nucleation at lower supersaturation is beneficial in the control the nucleation rate and the nucleation quantity and hence crystal size. A critical nucleus, that is just becoming stable in the

solution, could be a miniature crystal, nearly perfect in form, or a rather diffuse body with molecules in a state similar to that in the bulk liquid. Thermodynamic considerations indicate that the work to nucleate in solution must be equal to or larger than the energy barrier of nucleation which itself is proportional to T^{-2} and $(\ln S)^{-2}$ where T is temperature and S the supersaturation ratio [39]. Ultrasonic energy propagates in the form of longitudinal waves formed by alternate regions of compression and rarefaction of the liquid particles that result in the formation of cavitation bubbles. The collapse of these cavitation bubbles generates very high local temperatures and pressures with heating and cooling rates associated with each bubble greater than 109 K/s. The instant increase in pressure and temperature will cause local fluctuation of solution concentration and temperature. In the fluctuation regions, the critical potential barrier for nucleation lowers temporarily due to increasing in T and S, and so nucleation will be favored [40].

1.8.2. Effect of ultrasound on the reduction of agglomeration

Sonication can reduce the agglomeration via two pathways. One is the control of the magnitude of the primary nucleation number. The nucleation number per unit volume may determine whether agglomeration occurs. The second is the enhanced distribution of nuclei and improvement in the environment of the growing crystal. Observation with the naked eye suggests that the insonated crystal slurry is in a state of gas-liquid-solid co-existence where the crystal grains are in good suspension and remain discretely dispersed. This may be explained by the production of a local supercritical gas–liquid state through the high temperature and high pressure developed by the implosion of the cavitation bubble. After the crystal grains precipitate, the solution is very clear, which indicates complete chemical reaction and good crystallization.

The deposition of metals under the influence of ultrasound has received significant attention, particularly in the applied literature, as sonication is thought to confer various benefits over conventional silent electrodeposition. These are claimed to include increased deposit hardness, enlarged film thickness, improved deposition rates and efficiencies and greater adhesion of the deposit to the electrode [40].

1.8.3. Grain size

Ultrasonic agitation doesn't appear to have any specific effect on the grain size of electrodeposits. The change depends upon the metal being deposited the experimental

conditions such as current density, and the frequency and intensity of the ultrasonic field. Ultrasonic agitation reduces cathodic polarization during electrodeposition.Therefore deposits produced in an ultrasonic field should have larger grain size than those formed in static electrolyte. Rummel and Schmitt observed an increase in the grain size of copper deposits from an acid sulphate electrolyte ($CuSO4.5H_2O$ 200 g/l, H_2SO4 30 g/l) when subjected to an ultrasonic field (f = 330 kHz). Similarly, Kozan' found that ultrasonic agitation (f = 20 kHz) favoured the formation of coarse grained deposits from a Watts bath at current densities in the range of 200-1000 Am^{-2} and Roll reported that ultrasound (f= 34 kHz, I = 3 x 10s Wm^{-2}) produced large grained silver deposits from cyanide electrolytes at a current density of 200 Am^{-2}. Bondarenko and co-workers have indicated that changes in the magnitude and rate of cathodic passivation may be responsible for the contradictory results. Passivation favours the formation of nuclei and consequently fine grained deposits, whereas a decrease in concentration polarization at the cathode surface reduces nucleation and gives coarse grained deposits. Ultrasonic agitation of the solution reduces the increase in alkalinity of the catholyte during plating so that less hydroxide is precipitated and also disperses the hydroxide and lowers the sedimentation rate by a factor of ten. These effects decrease the number of nuclei and consequently coarser grained deposits are formed. At higher current densities the PH change, even with ultrasound, is greater so that more precipitation occurs and finer grained deposits are produced.

Barnartt proposed that the effect of ultrasound on grain size is the result of two opposing processes. The first is the violent agitation which reduces the concentration polarization and promotes the formation of larger grains and the second is the high frequency mechanical vibration which may induce prolific nucleation in the depositing metal resulting in a finer grain size [41, 42].

1.8.4. Hardness

It is widely accepted that ultrasonic agitation increases the hardness of the electrodeposited metal thin film. Ultrasonic agitation produces finer grained deposits and that smaller grain size and packing density plays a major role in the variation of hardness. It is indicated that harder deposits have a smaller grain size. The higher hardness is due to the inclusion of an increased number of foreign particles in the deposits that can reduce the mobility of dislocations during deformation. Kelsens pointed out, however, that suspended

impurities in the electrolyte do not easily adhere to the cathode because it does not follow the movement of the particles but this may not apply if the intensity of the ultrasound drops below the cavitations threshold of the liquid. Below the cavitations threshold the variable sound pressure of the acoustic field becomes the controlling factor in any property change. Under these conditions no dispersion of the particles occurs, the cathode becomes passivated, a smaller grain size results and more particles are included in the deposit, which gives an increase in hardness. When the ultrasonic vibration is accompanied by cavitations dispersion occurs, the cathode is depassivated and the number of particles included decreases. The inclusion of hydrogen, which can result in lattice deformation, is not thought to be a primary factor in increasing the hardness because the amount contained in deposits formed under ultrasonic conditions has been found to be half that present in conventionally produced deposits. The fact that ultrasound decreases the internal stress in deposits cannot account for the increase in the hardness [42,43].

. **Table-2: Different hardness value for different materials under different conditions**

Plated Metal	Hardness HV(100g Load)		
	Conventional range	Air agitation	Ultrasonic agitation
Silver	55-80	88	104
Copper	35-190	167	248
Cadmium	15-60	36	84
Zinc	45-120	50	103

1.8.5. Residual stress

The effects of ultrasonic agitation on the residual stress of electrodeposits are contradictory. Because ultrasound has been shown to reduce the amount of hydrogen occluded in electrodeposit and hydrogen is considered to be a possible cause of residual stress in electrodeposits, it follows that ultrasonic agitation should reduce the residual stress in metals that are codeposited with hydrogen. It is found that both the amount of hydrogen and the residual stress are reduced in nickel deposits when ultrasonic agitation is used.

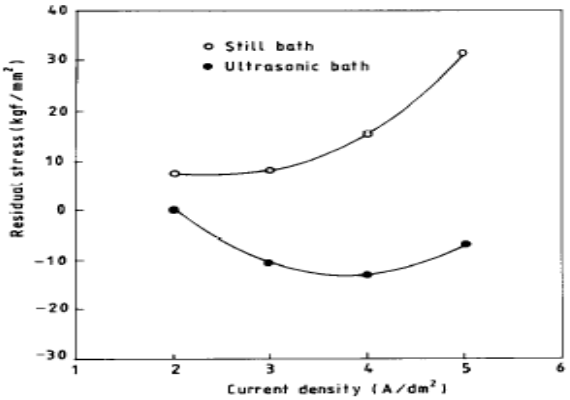

Fig-1.18: Residual stresses of nickel electrodeposits.

This decrease in the stress has been recorded for chromium and nickel. Zaidmans' has suggested that the increase in the internal stress in iron deposits caused by ultrasonic agitation can be explained by the following factors: a decrease in the change of the pH in the catholyte, the desorbing action of ultrasound, a decrease in the grain size and an increase in the microdistortion and dislocation content in the coating [44].

1.8.6. Porosity

The reduction in porosity achieved by ultrasonic agitation caused by the accelerated removal of hydrogen from the cathode surface during plating. This allows uniform deposition to occur and prevents the formation of pores in the coating where the substrate is shielded from deposition by hydrogen bubbles. As well as hydrogen effect the ultrasonic field causes the formation of fined grained, densely packed deposits which has low porosity. The second effect probably accounts for the reduction in porosity in metals , which are not codeposited with hydrogen, although the depassivating action of ultrasound may also contributing to reduced porosity.

1.8.7. Brightness

Electrodeposits formed in an ultrasonic field are brighter than those produced at identical current densities under conventional conditions. The current density at which bright coatings are initially deposited and the degree of brightening increases as the intensity of the acoustic field is raised. The increased brightness generally exhibited by coatings produced in an ultrasonic field is normally associated with a small deposit grain size and higher packing

density. For example Kochergin and Vyaseleva investigated the effect of ultrasonic vibration on the brightness of nickel deposits. They observed that during electrodeposition the surface of the cathode is depassivated and the resulting deposit has a finer grain size and higher grain packing density, but the texture is less perfect. Thus they concluded that the increase in the brightness of electrodeposits resulting from ultrasonic vibration is caused by the formation of small grained deposits.

1.9. Objective of the work

- Synthesis of the copper thin film in sonoelectrodeposition route by varying acid concentaration, temperature and copper concentration.
- Characterization of the deposited film by XRD, SEM, AFM, DSC and mechanical properties by nanoidentation.
- Study the surface morphology and mechanical properties.

Chapter-2

Experimental

&

Characterization

CHAPTER 2

2. Experimental & Characterization

2.1. Instrumentation

The experiments were done with ECOCHEMIE Autolab PGSTAT 12 potentiostat system and three electrode electrochemical cell. The working electrode was a Cu-plate; the counter electrode was an aluminum plate and Ag/AgCl worked as reference electrode. Before each scan and subsequent experiments, electrodes were polished, washed and dried properly. For sonoelectrochemical experiment ultrasonic vibrator of frequency (30 KHz) was used, which was positioned just below the electrochemical cell. The arrangement is shown in figure 2.1.

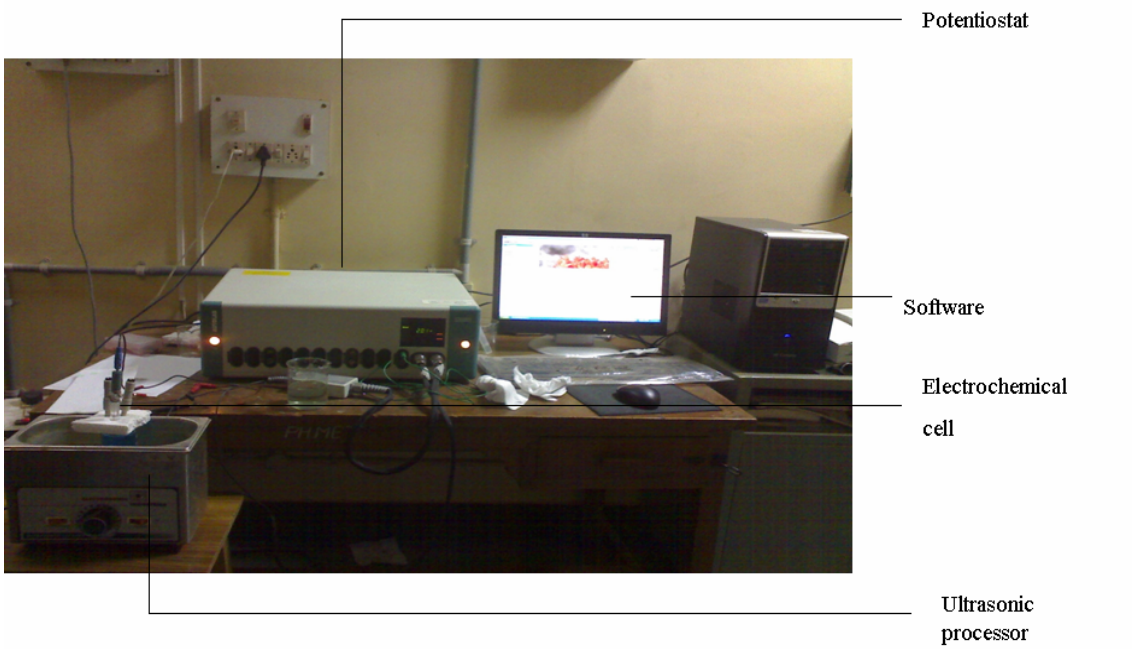

Fig. 2.1. Experimental Set up

2.2. SYNTHESIS

Electrodeposition is used as a route to fabricate copper thin film. The deposition was commenced in potentiostatic mode. Synthesis was done in an aqueous medium. The metallic system is coffined to mainly copper. The bath used is a sulfate bath. Doubly distilled water and analytical grade chemicals were used supplied by nice chemicals. The operating parameters are, a varying copper ion concentration of 10 g l^{-1}, 20 g l^{-1}, 30 g l^{-1}, 40 g l^{-1} and 50 g l^{-1}, varying P^H with sulphuric acid like 40 g l^{-1}, 60 g l^{-1}, 80 g l^{-1}, 100 g l^{-1}, and120 g l^{-1} in silent as well as ultrasonic condition at room temperature. After that by fixing the concentration of copper sulphate to 10 g l^{-1} and sulphuric acid 60 g l^{-1}, the copper thinflim is prepared by varying the temperature like 25 ˚C, 20 ˚C, 15 ˚C, 10 ˚C, 5 ˚C, −1 ˚C and −3 ˚C in both silent and ultrasonic condition. Power supply was done with EG&G 273 potentiostat/galvanostat system in potentiostatic condition. Electrochemical cell is s three electrode systems with aluminum substrate as working electrode, copper plate is as counter electrode and saturated calomel electrode as reference electrode. The electrolytic solution and the three electrodes were taken in a glass beaker. For sonication impact an electrosonic ultrasonic cleaner, model no. EI 2 LH, of 30 kHz, 60 Watt power was used. The glass jar was then put in a ultrasonic vibrator. The applied potential sweep is 300 mV to 600 mV at a scanning rate of 1 mV/s. After dissolution of copper plate, deposition of copper thin film is done on the aluminum plate. Before each scan and subsequent experiments, electrodes were polished, washed and dried properly. To increase the reaction rate and avoid the powder deposits the solution was agitated by using a ultrasonic vibrator of frequency 30KHZ.

2.3. Characterization Technique

Several techniques have been used to characterize the electrodeposits and sonoelectrodeposits of copper thin film. The X-ray diffraction, in the range of scanning angel 30-150˚ at a scanning rate 2˚ with CuKα radiation (λ=1.5406A^0) using Philips X' PERT System X-Ray Diffractometer. JEOL scanning electron microscope (SEM) at low acceleration voltages, atomic force microscope (AFM) were employed to examine the morphology, particle size and microstructure of the electrodeposits and sonoelectrodeposits of thin film at the various temperatures. The chemical composition/purity of the electrodeposits and sonoelectrodeposits was determined by energy dispersive spectroscopy (EDS) analysis. Mechanical properties were

studied by nanoindentation. Specific data were recorded by a low temperature METTLER TOLEDO DSC 822^e.

2.3.1. X-RAY Diffraction

X-ray scattering techniques are a family of non-destructive analytical techniques which reveal information about the crystallographic structure, chemical composition, and physical properties of materials and thin films.

These techniques are based on observing the scattered intensity of an x-ray beam hitting a sample as a function of incident and scattered angle, polarization, and wavelength or energy [45]. The mechanical assembly that makes up the sample holder, detector arm and associated gearing is referred to as goniometer. The working principle of a Bragg-Brentano para focusing (if the sample was curved on the focusing circle we would have a focusing system) reflection goniometer is explained below. The distance from the X-ray focal spot to the sample is the same as from the sample to the detector. If we drive the sample holder and the detector in a 1:2 relationship, the reflected (diffracted) beam will stay focused on the circle of constant radius [45]. The detector moves on this circle.

The crystallite size and lattice strain in the powder particles can be determined by the X-ray peak broadening techniques. X-ray diffraction peaks are broadened due to [46]:

1. Instrumental effects,
2. Small particle size,
3. Lattice strain in the material.

However, if one is interested only in following the trend of change of crystallite size with milling conditions, this simple technique may be acceptable. While the X-ray peak broadening due to small crystallite size is inversely proportional to cosθ. The crystallite size is determined by measuring the Bragg peak width at half the maximum intensity and putting its value in scherrer's formula. The crystallite size and lattice strain in the powder particles can be determined by the X-ray peak broadening techniques. Using the method developed by Williamson and Hall [47], the contributions of the particle size and strain to be observed X-ray line broadening, β , are considered to be additive.

$$\beta_{total} = \beta_{particlesize} + \beta_{strain}$$

The contribution of broadening due to small particle size is given by Scherrer equation while the broadening due to strain is represented by differentiation of Bragg's law.

$$\beta_{total} = \frac{.94\,\lambda}{t\cos\theta} + 4\tan\theta\left(\Delta d/d\right)$$

The total broadening (β_{total}) is the measured FWHM total in radians, corrected for instrumental broadening. The X-ray wavelength of the source (CuKa0.154nm) is given by λ, *t* is the particle size, and $\Delta d/d$ represents the strain. Multiplying both sides of the above equation by cos θ gives the final form,

$$\beta_{total}\cos\theta = \frac{.94\,\lambda}{t} + 4\tan\theta\left(\Delta d/d\right)$$

which is used to calculate the particle size and strain for copper from a plot of $\beta_{total}\cos\theta$ versus sin θ. Data are taken with a

2.3.2. Scanning Electrone Microscope

The scanning electron microscope (SEM) is a type of electron microscope that images the sample surface by scanning it with a high-energy beam of electrons in a raster scan pattern. The electrons interact with the atoms that make up the sample producing signals that contain information about the sample's surface topography, composition and other properties such as electrical conductivity.

In a typical SEM, electrons are thermionically emitted from a tungsten filament cathode and are accelerated towards an anode. Tungsten is normally used in thermionic electron guns because it has the highest melting point and lowest vapor pressure of all metals, thereby allowing it to be heated for electron emission. Other electron sources include lanthanum hexaboride (LaB6) cathodes, which can be used in a standard tungsten filament SEM if the vacuum system is upgraded. Electrons can also be emitted using a field emission gun (FEG).

The electron beam, which typically has an energy ranging from a few hundred eV to 40 keV, is focused by one or two condenser lenses into a beam with a very fine focal spot sized 0.4 nm to 5 nm. The beam passes through pairs of scanning coils or pairs of deflector plates in the electron column, typically in the final lens, which deflect the beam horizontally and vertically so

that it scans in a raster fashion over a rectangular area of the sample surface. When the primary electron beam interacts with the sample, the electrons lose energy by repeated scattering and absorption within a teardrop-shaped volume of the specimen known as the interaction volume, which extends from less than 100 nm to around 5 μm into the surface.

The size of the interaction volume depends on the electron's landing energy, the atomic number of the specimen and the specimen's density. The energy exchange between the electron beam and the sample results in the reflection of high-energy electrons by elastic scattering, emission of secondary electrons by inelastic scattering and the emission of electromagnetic radiation which can be detected to produce an image [47].

2.3.3: Energy dispersive X-Ray analysis

EDX Analysis stands for Energy Dispersive X-ray analysis. It is sometimes referred to also as EDS or EDAX analysis. It is a technique used for identifying the elemental composition of the specimen, or an area of interest thereof.

The EDX analysis system works as an integrated feature of a scanning electron microscope (SEM), and cannot operate on its own without the latter. During EDX Analysis, the specimen is bombarded with an electron beam inside the scanning electron microscope. The bombarding electrons collide with the specimen atoms' own electrons, knocking some of them off in the process. A position vacated by an ejected inner shell electron is eventually occupied by a higher-energy electron from an outer shell. To be able to do so, however, the transferring outer electron must give up some of its energy by emitting an X-ray. The amount of energy released by the transferring electron depends on which shell it is transferring from, as well as which shell it is transferring to. Furthermore, the atom of every element releases X-rays with unique amounts of energy during the transferring process. Thus, by measuring the amounts of energy present in the X-rays being released by a specimen during electron beam bombardment, the identity of the atom from which the X-ray was emitted can be established.

The output of an EDX analysis is an EDX spectrum. The EDX spectrum is just a plot of how frequently an X-ray is received for each energy level. An EDX spectrum normally displays peaks corresponding to the energy levels for which the most X-rays had been received. Each of these peaks is unique to an atom, and therefore corresponds to a single element. The higher a peak in a spectrum, the more concentrated the element is in the specimen [47].

An EDX spectrum plot not only identifies the element corresponding to each of its peaks, but the type of X-ray to which it corresponds as well. For example, a peak corresponding to the amount of energy possessed by X-rays emitted by an electron in the L-shell going down to the K-shell is identified as a K-Alpha peak. The peak corresponding to X-rays emitted by M-shell electrons going to the K-shell is identified as a K-Beta peak.

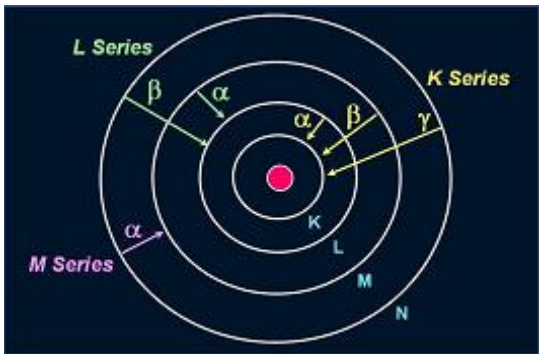

Fig.2.2. Elements in an EDX spectrum are identified based on the energy content of the X-rays emitted by their electrons as these electrons transfer from a higher-energy shell to a lower-energy one

2.3.4. Atomic Force Microscope

The atomic force microscope (AFM) or scanning force microscope (SFM) is a very high-resolution type of scanning probe microscope, with demonstrated resolution of fractions of a nanometer, more than 1000 times better than the optical diffraction limit

The AFM consists of a microscale cantilever with a sharp tip (probe) at its end that is used to scan the specimen surface. The cantilever is typically silicon or silicon nitride with a tip radius of curvature on the order of nanometers. When the tip is brought into proximity of a sample surface, forces between the tip and the sample lead to a deflection of the cantilever according to Hooke's law. Depending on the situation, forces that are measured in AFM include mechanical contact force, Van der Waals forces, capillary forces, chemical bonding, electrostatic forces, magnetic forces (see Magnetic force microscope (MFM)), Casimir forces, solvation forces etc. Typically, the deflection is measured using a laser spot reflected from the top of the cantilever into an array of photodiodes. Other methods that are used include optical interferometry, capacitive sensing or piezoresistive AFM cantilevers. These cantilevers are fabricated with piezoresistive elements that act as a strain gauge. Using a Wheatstone bridge, strain in the AFM cantilever due to deflection can be measured, but this method is not as sensitive as laser deflection or interferometry.

If the tip were scanned at a constant height, there would be a risk that the tip would collide with the surface, causing damage. Hence, in most cases a feedback mechanism is employed to adjust the tip-to-sample distance to maintain a constant force between the tip and the sample. Traditionally, the sample is mounted on a piezoelectric tube, that can move the sample in the z direction for maintaining a constant force, and the x and y directions for scanning the sample. Alternatively a 'tripod' configuration of three piezo crystals may be employed, with each responsible for scanning in the x, y and z directions. This eliminates some of the distortion effects seen with a tube scanner. The resulting map of the area s = f(x, y) represents the topography of the sample.

2.3.5. Nanoindentation

In nanoindentation small loads and tip sizes are used, so the indentation area may only be a few square micrometres or even nanometres. This presents problems in determining the hardness, as the contact area is not easily found. Atomic force microscopy or scanning electron microscopy techniques may be utilized to image the indentation, but can be quite cumbersome. Instead, an indenter with a geometry known to high precision (usually a Berkovich tip, which has three-sided pyramid geometry) is employed. During the course of the instrumented indentation process, a record of the depth of penetration is made, and then the area of the indent is determined using the known geometry of the indentation tip. While indenting various parameters, such as load and depth of penetration, can be measured. A record of these values can be plotted on a graph to create a load-displacement curve (such as the one shown in Figure 2.3). These curves can be used to extract mechanical properties of the material.

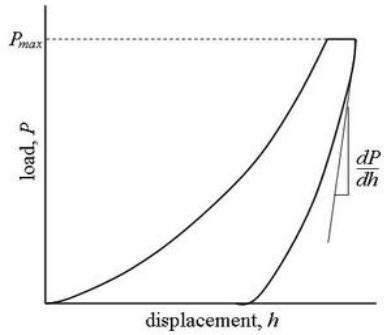

Fig.2.3.Schematic of load-displacement curve for an instrumented nanoindentaion test

The hardness and modulus were obtained from the load displacement data following the procedure proposed by Oliver and Pharr, which will be briefly described below. The definition of hardness is

$$H=P_{Max}/A$$

where P_{Max} is the maximum load and A is the projected area of the impression. The projected area is determined from the indenter tip calibration and is a function of the contact depth, h_c.

The contact depth was derived from the initial slope S=dP/dh, of the first 50% of the last unloading curve and can be expressed

$$H_c = h_{Max} - \varepsilon \frac{P_{Max}}{S}$$

where ε is the indenter constant (0.75 for a Berkovich tip) and h_{max} is the total displacement under maximum load. The stiffness S contains information of the modulus of the sample

$$S = \frac{dp}{dh} = \frac{2}{\sqrt{\pi}} E_r \sqrt{A},$$

where E_r is the reduced modulus due to non-rigid indenter. The modulus of the sample is obtained from the following equation

$$\frac{1}{E_r} = \frac{(1-\gamma^2)}{E} + \frac{(1-\gamma_i^2)}{E_i},$$

where E and γ are Young's modulus and Poisson's ratio, respectively, for the specimen, and E_i and γ_i are the corresponding values for the indenter[49].

2.3.6. Specific heat measurement

The property was studied with a low temperature DSC (Differential Scanning Calorimeter). The program was set with a dried alumina powder. A 5 minutes isothermal run has given at 35˚C, and then a dynamic cycle run from 35˚C to 300˚C and finally an isothermal run for 5 minutes at 300˚C. The process was repeated for the whole samples and the data is presented somewhere else in chapter 3.

Chapter-3

Results & Discussion

CHAPTER 3

3. Results and Discussion

3.1. Effect of temperature

3.1.1. Electrochemical LSV analysis

Figure 3.1 represents the linear sweep voltametry for the deposits at various temperatures for both the conditions.

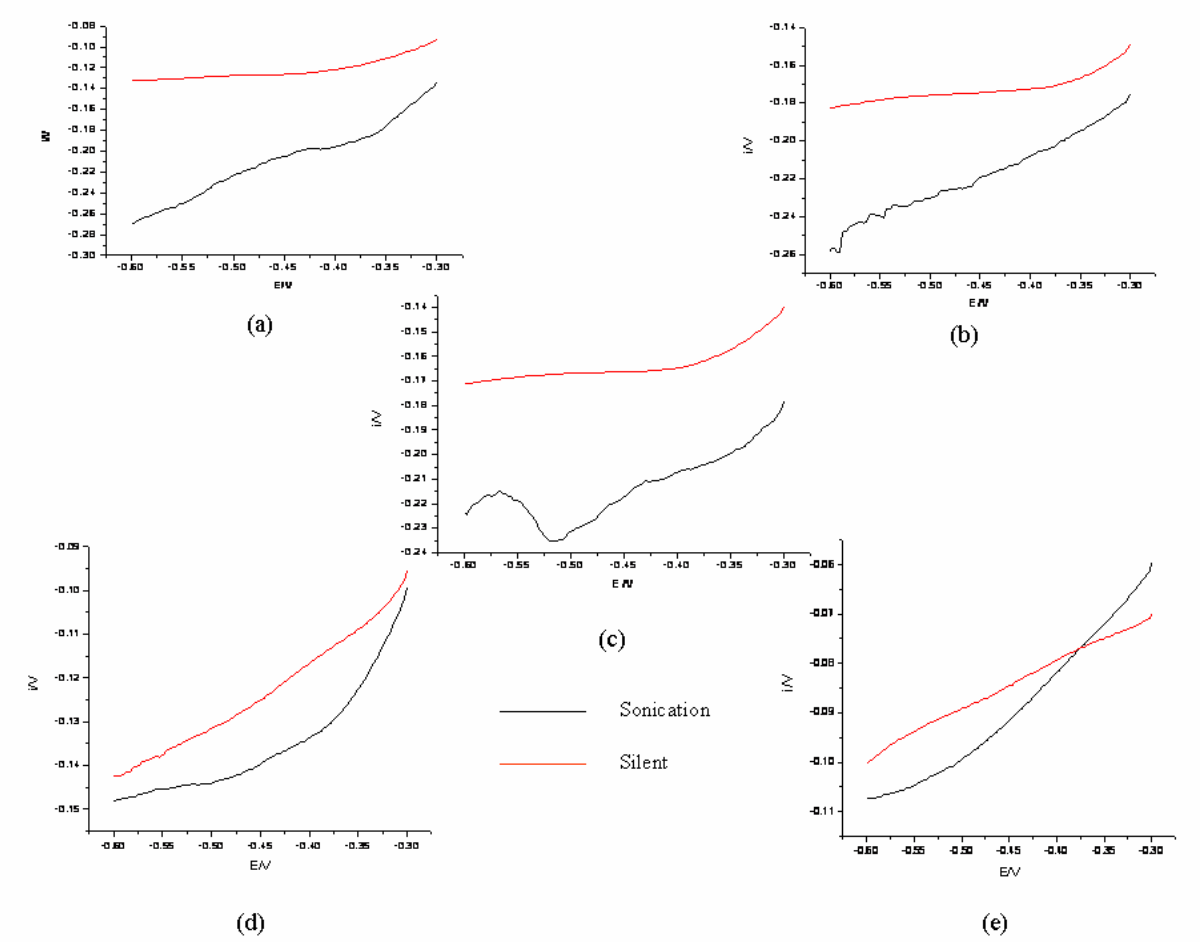

Fig. 3.1. LSV for copper deposits at (a) 25˚C, (b) 20˚C, (c) 15˚C, (d) 10˚C, (e) 5˚C

It can be observed that the amount of electricity passed decreases with decreasing temperature for both the conditions. The regime of the slopes for silent conditions are flat indicating instatntaneous nucleation where as for ultrasonic conditions the graphs are having steep slopes, so that nucleation occurs through out the process i.e. progressive nucleation. This observation indicates that the deposit should be compact and fine grained at low temperatue as compared to the silent one. The above mentioned fact can be clarified in the next section of phase and structure analysis.

3.1.2. Phase and structure analysis

Fig 3.1 and 3.2 represents the XRD pattern of copper deposits at various bath temperatures like 25˚C,20˚C,15˚C,10˚C,5˚C in both silent and ultrasonic condition. The peaks show high crystallinity of copper with some aluminium peaks because of the substrate.

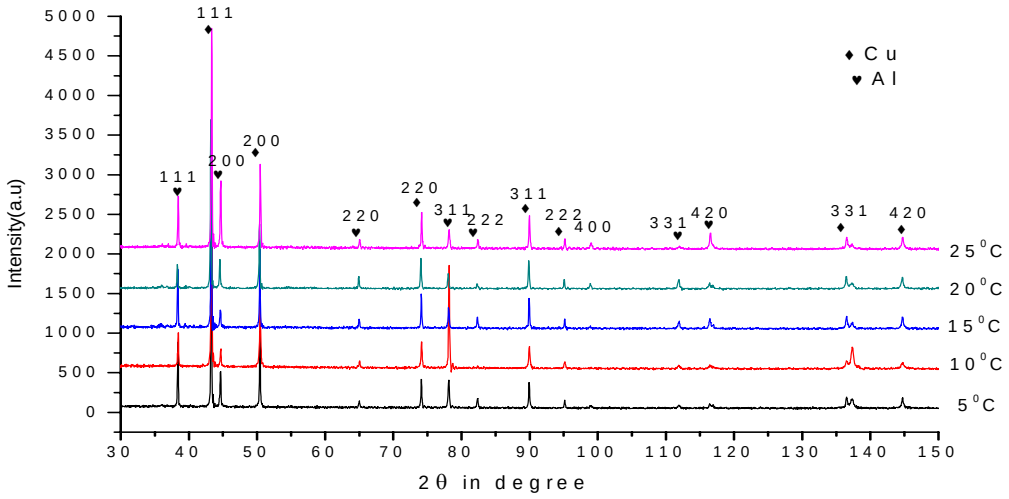

Fig.3.2. XRD patterns of thin film copper electrodeposits by varying temperature (silent condition)

The diffraction peaks at 2θ = 43.27, 50.34 can be indexed as the [111], [200] planes of copper with cubic symmetry respectively (JCPDS card no. 04-0863). With decreasing temperature, broadening increases where as intensity decreases. The broadening of peaks can be attributed to small particle size and strain of crystalline materials. Peaks from (311) and (222) planes are present in all deposits. Whereas the peak corresponding to the plane (400) at 2θ of 116.923 is not present in graphs. The above result supports the fact that diffraction from planes at high angle is

not prominent with reduced grain size. By decreasing the temperature the crystal size also reduces from70.44nm to45.99nm.

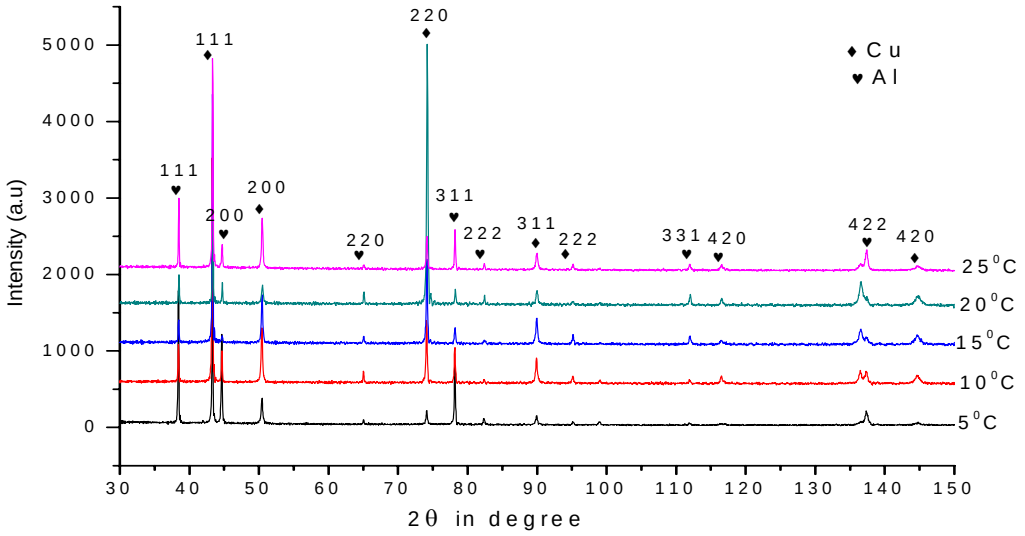

Fig.3.3. XRD patterns of thin film copper electrodeposits by varying temperature (ultrasonic condition)

Fig. 3.4. shows the SEM analysis of the samples at various temperatures in both the conditions. It can be observed for fig. 3.1. (b) that the deposit at ambient condition is giving a clear impression of powdery morphology, while the grains are not uniform. Fig.3.4. (a) shows the corresponding figure at silent condition. The deposit is a highly branched sharp dendritic structure. Deposit at 20˚C temperature is shown in fig. 3.4.(c) and (d). Sonicated substrateis covered by closely spaced copper structures as comparison to that of the truncated dendrites of the deposit withot ultrasound. Significant change in appearance can be observed in fig.3.4. (e) and (f) at 15˚C. The basic characteristic of morphology is a uniform copper covered surface with well agglomerated spheroids. The above result is attributed to the following facts. First, low temperature has resulted high supersaturation favoring formation of smaller nuclei but in a random fashion of discharging. Second**,** ultrasound has helped in rate of mass transportation thus creating enhanced nucleation. This effect has filled the gap between two adjacent nuclei leading to a compact mass. Sonicated deposits are well covered

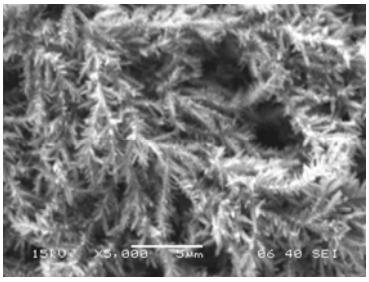
(a)

(25˚C)

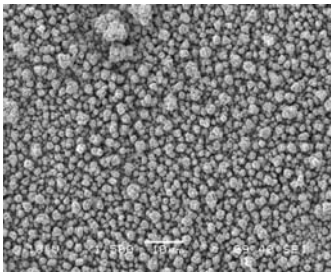
(b)

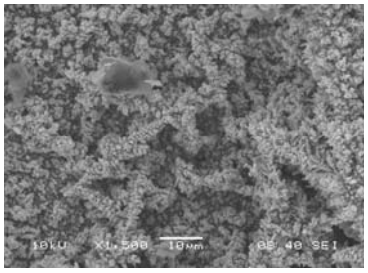
(c)

(20˚C)

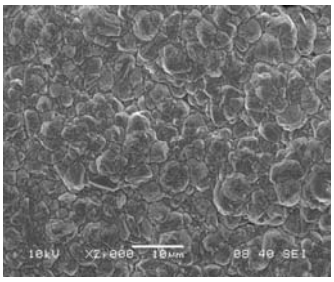
(d)

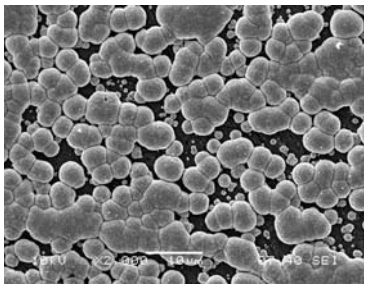
(e)

(15˚C)

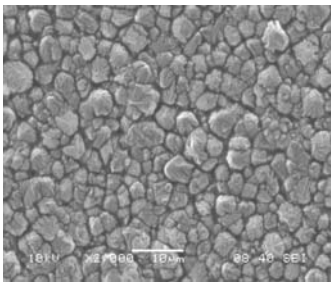
(f)

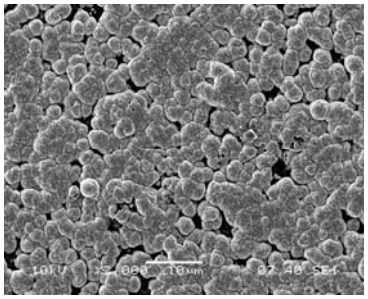
(g)

(10˚C)

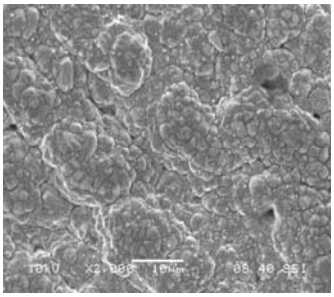
(h)

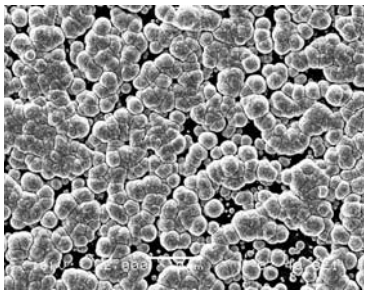
(i)

(5˚C)

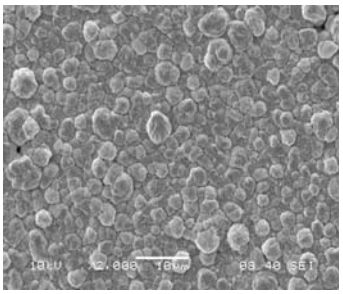
(j)

(Silent)

(Sonication)

Fig. 3.4. SEM micrographs of copper deposits

than the silent deposits confirming higher throwing power and current efficiency even at low temperature. Height mode topographical AFM micrographs of the deposits at 25˚C , 15˚C, 5˚C are shown in fig.3.5. The deposit at 25˚C is copper spheroids and the surface is nonuniform as confirmed by the phase image of the deposit. Because the surface is uniform, it is reasonable to estimate a 2D growth onto the 2D substrate. The 3D roughness image of the deposits show the decreasing roughness with temperature.

Table 3.Composition analysis at different temperature

Temperature	Silent Composition (at%)			Sonication Composition (at%)		
	Cu	O	S	Cu	O	S
25	76.38	20.62	3	100	-	-
20	72	25.90	2.10	100	-	-
15	65.05	33.72	1.23	100	-	-
10	61.85	37.12	1.03	100	-	-
5	54.5	45	0.5	100	-	-

A comparative compositional analysis form the EDS result has given in table 2. The results shows that with decreasing temperature the impurity levels mainly at% of oxygen is increasing in silent deposit where as sonication depositions have zero levels of contamination. Oxygen content has got increased roughly with decreased temperature. EDS plot of the above mentioned fact has been given in fig. 3.6. Compound analysis from the Oxford data has shown that the oxides at high temperatures are mainly CuO where as at low temperatures these are mainly Cu_2O. The fact that ionic character tends to increase [50] with reducing grain size and high symmetry structures are stable at low temperatures [51] might have resulted the above compositional variation in silent conditions.

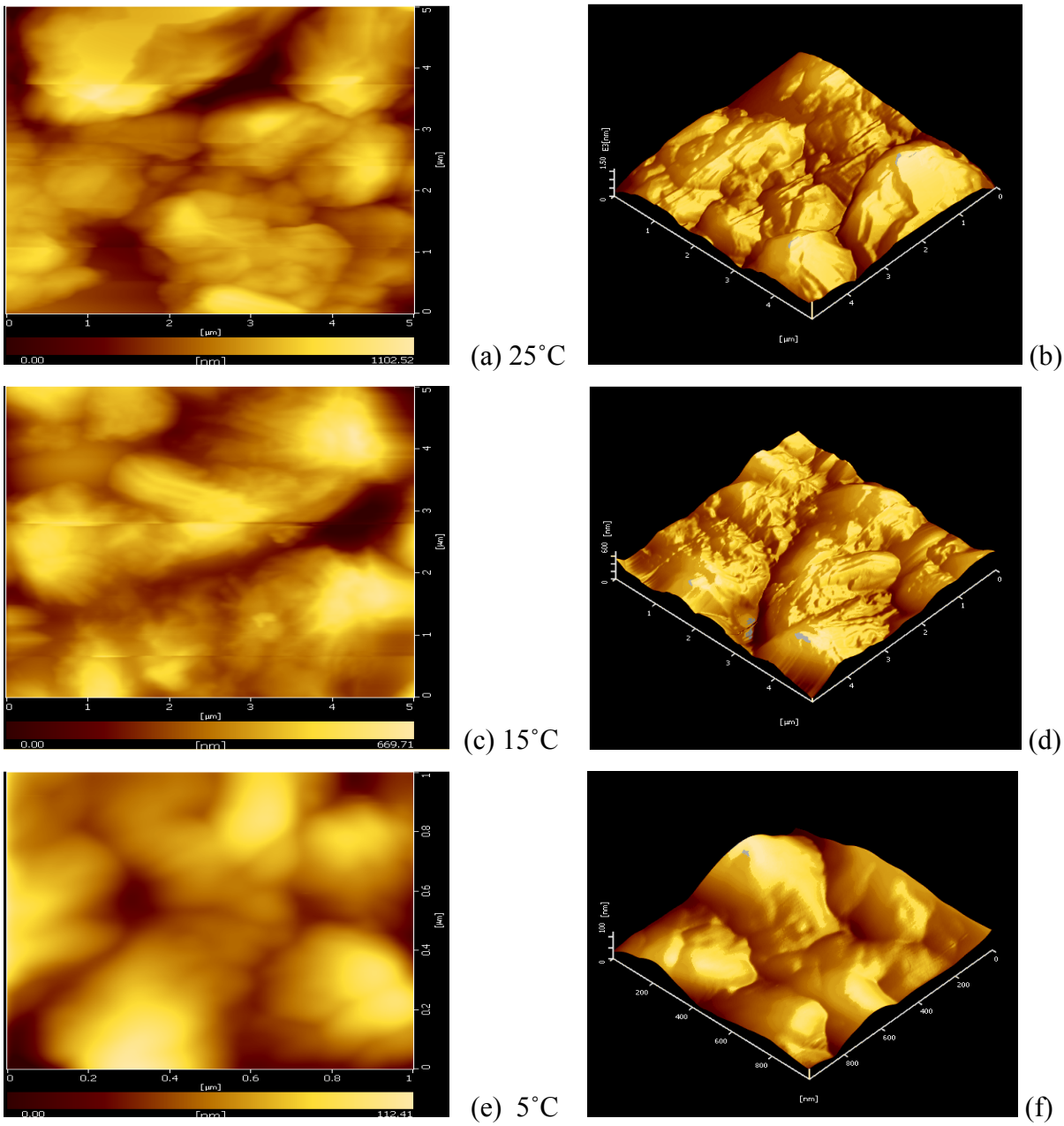

Fig. 3.5. AFM image of sonicated copper deposits

Sulfur content of the deposit also shows a decreasing trend with temperature. Sulfur usually gets adsorbed on the substrate form the electrolyte. Low temperature has reduced the adsorption tendency of the same. In sonication conditions the formation of the above weak covalent bond between copper and oxygen might have not been possible in the presence of a highly dynamic energy system. Due to in situ cavitational cleaning of the electrodes, the deposit obtained is purest in its form and free form adsorbed sulfur unlike the deposit in silent condition.

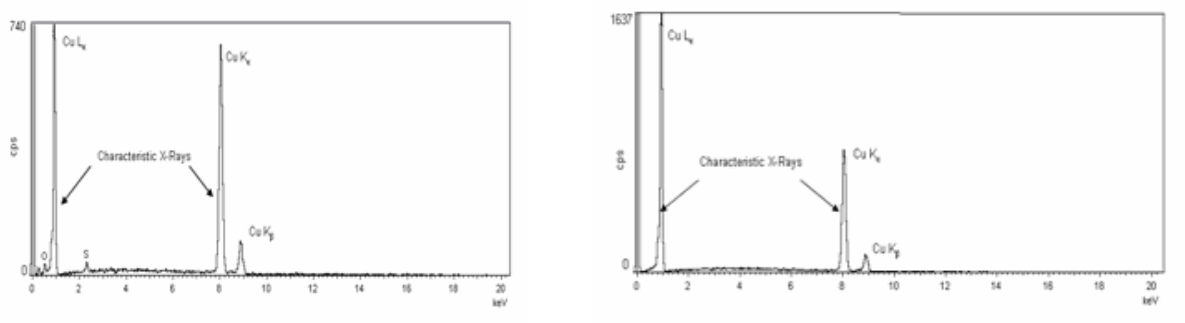

(Silent) (Sonication)

Fig. 3.6. EDS plot of the copper deposits at 25°C

3.1.3. Heat capacity measurement

Fig. 3.7. shows the specific heat measurement data for the films. The scale is represented in exothermic setting. The procedure followed for the above mentioned result has been Mentioened some where else in the experimental section. It can be observed that the heat absorved with decreased temperature increases. Decrease in grain size the surface entropy increases, and when extra amount of heat supplied to the materials it gets dissipated in the materials as stored energy. So when the experiments conducted for the above materails, the amount of heat absoreved increase from 2 to 8 mW.

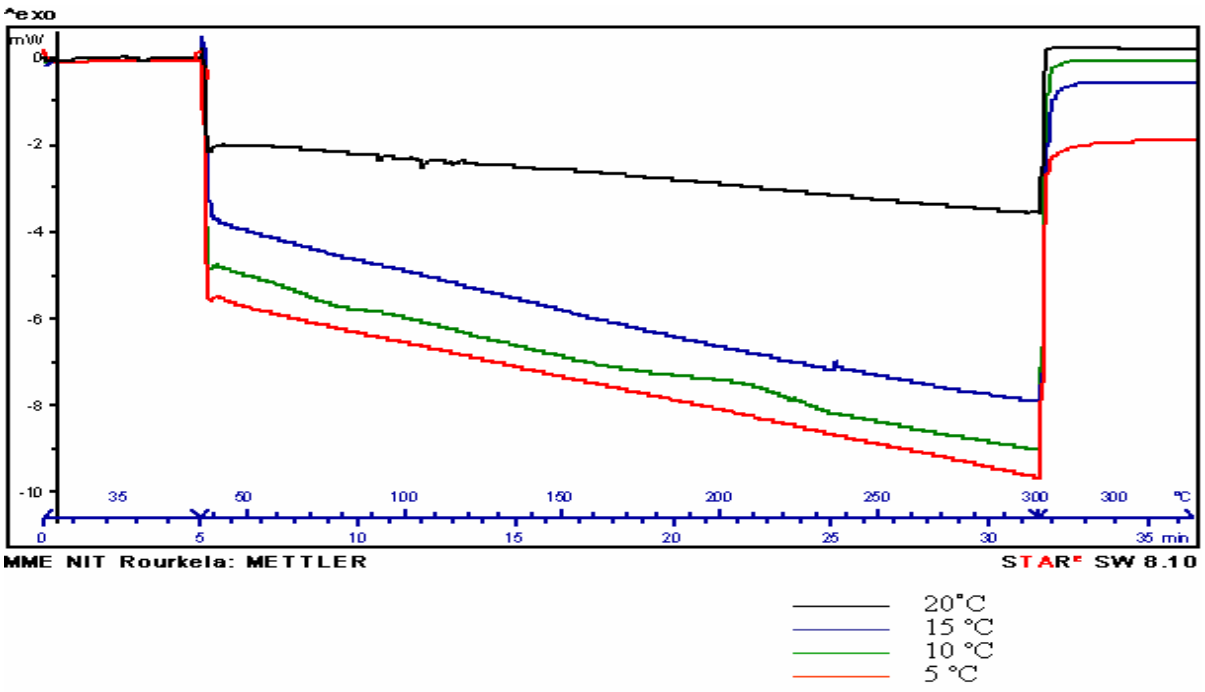

Fig. 3.7. DSC plot of heat capacity for copper thin films

3.1.4. Hardness characteristics

Figure 3.8.shows the hardness characteristics of the deposit at various temperatures. The tests are done with a constant load applied to the substrate and the displacement is recorded for each of the temperatures.

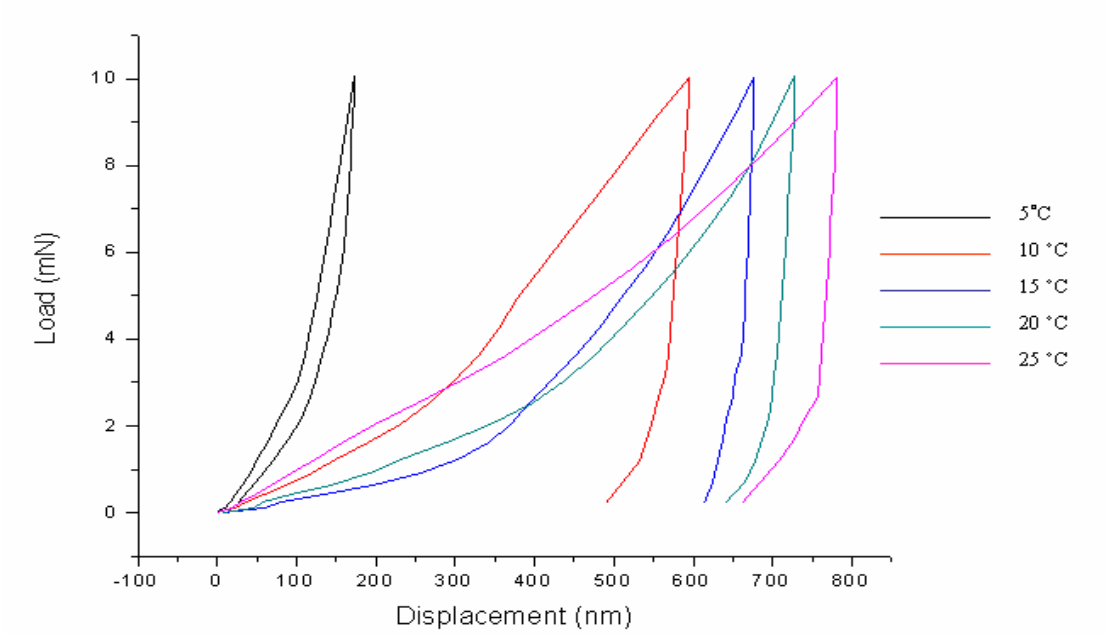

Fig. 3.8. Load-Displacement data of copper thin films

The fixed force applied is 10 mN. It can be seen that the displacement decreases with decreasing temperature. The conventional Hall-Petch equation, hardness/yield strength increses as $H = H_o + kd^{-1/2}$, is followed from the above observation. The fact can be explained as dislocation which moves from one grain into another has to adjust its direction with increasing number of grain boundaries.Thus it can be inferred that the more grains a material has, the more difficult for the dislocations to move. To put it in another way, the finer the grains are, the harder the material is.

3.2. Effect of acid concentration

3.2.1. XRD Analysis

The X-RD patterns of the sample synthesized at different acid concentrations both at silent and sonication conditions are shown in figs 3.9. and 3.10. respectively.

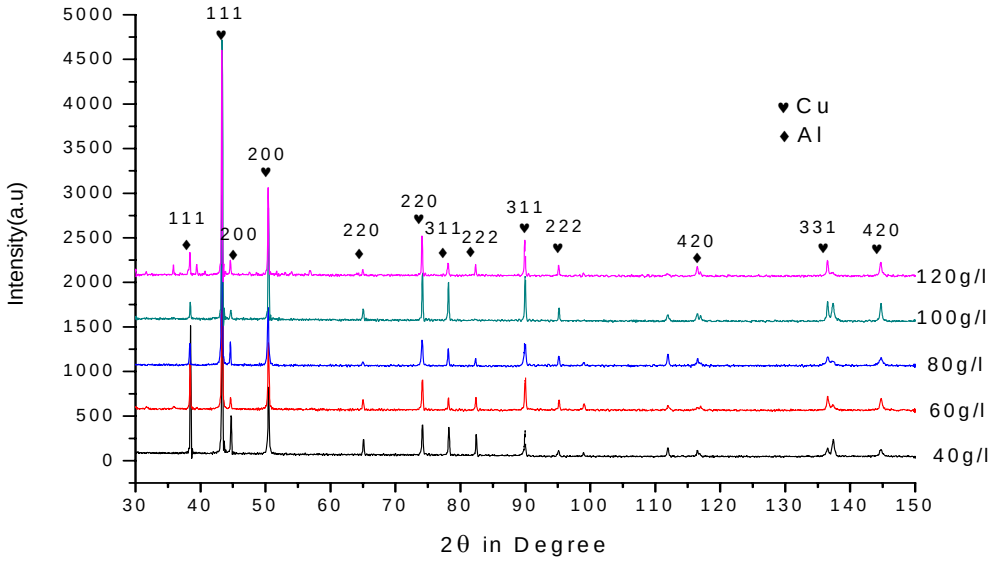

Fig.3.9. XRD patterns of thin film copper electrodeposits at different acid concentrations (silent condition)

It is observed that the entire XRD pattern consists of peaks corresponding to different crystallographic planes of cubic copper lattice. The XRD pattern revels that acid concentration of the bath strongly affects the formation of copper thin film. In the XRD patterns of all the films obtained at different acid concentration shows that, the peak corresponding to the plane (111),(200),and (220) are prominent as compared to (311),(222), (331) and(420) planes.

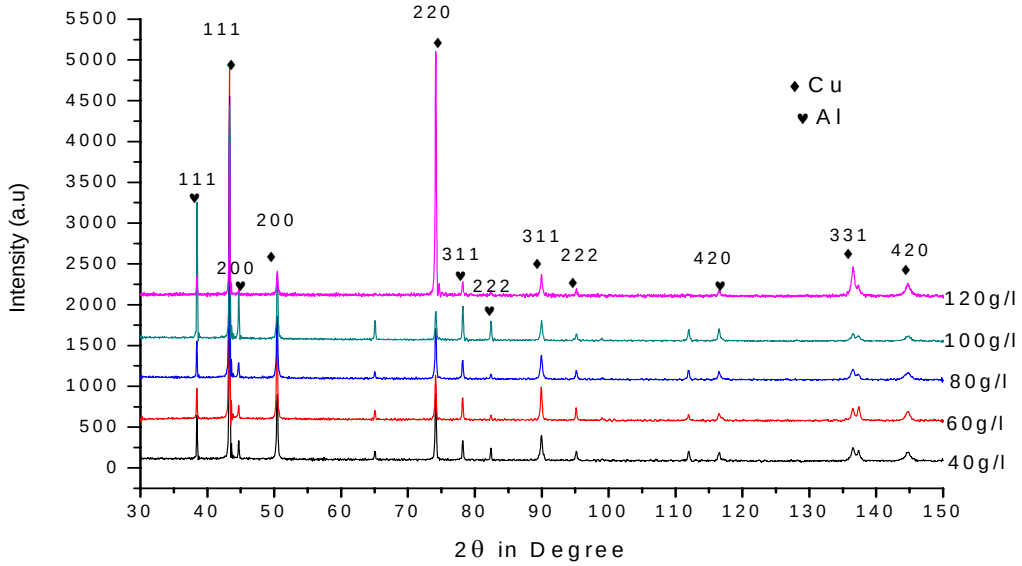

Fig.3.10. XRD patterns of thin film copper electrodeposits at different acid concentrations (ultrasonic condition)

A high peak intensity is observed at 60g/l acid concentration. Particle size is also calculated by using the Scherrer formula. It is observed that by increasing the acid concentration of the electrolytic bath the particle size reduces from 43.71nm to 34.65nm.

3.2.2. SEM Analysis

The Surface morphology of copper thin film deposited at different acid concentration in silent and ultrasonic condition are shown in fig 3.11. The effect of acid concentration on the surface morphology of copper deposits was studied by using SEM micrographs. The surface morphology is clearly seen to be strongly influenced by the acid concentration. The micrographs show that in silent condition by increasing the acid concentration means 40gpl to 120gpl, the nuclei population density increased on the surface but the growth rate is increased. In low acid concentration the surface is not uniform, the surface film looks like corncob structure but by increasing the acid concentration, the surface looks like uniform means nuclei population density increased but the growth rate is decreased which is shown in fig 3.11.

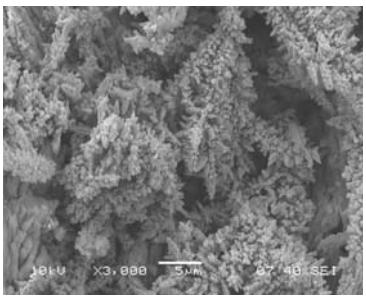
(a)

(40gl^{-1})

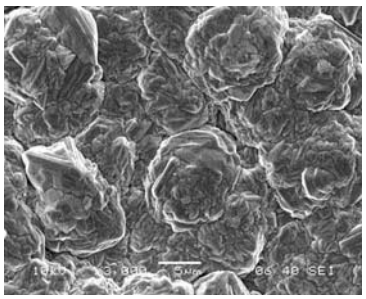
(b)

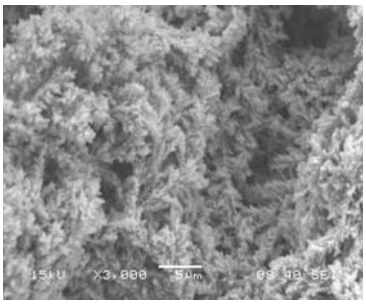
(c)

(60 gl^{-1})

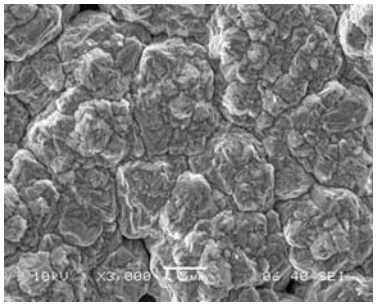
(d)

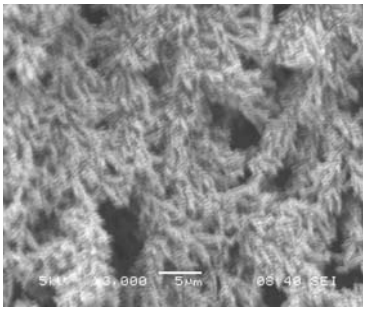
(e)

(80 gl^{-1})

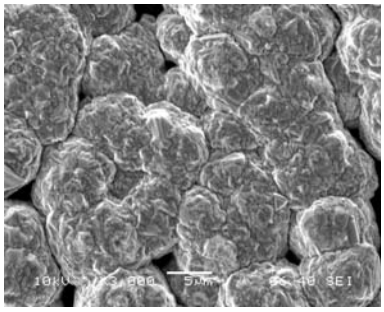
(f)

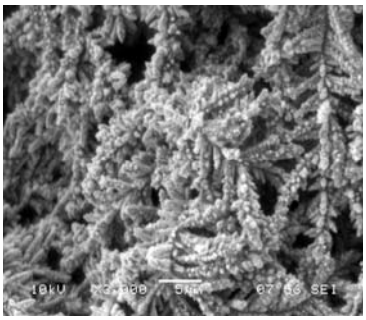
(g)

(100 gl^{-1})

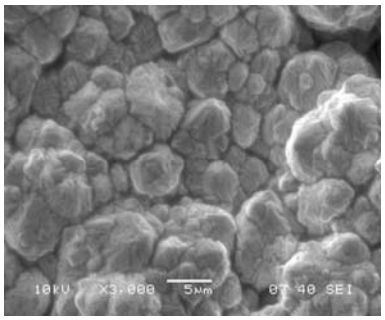
(h)

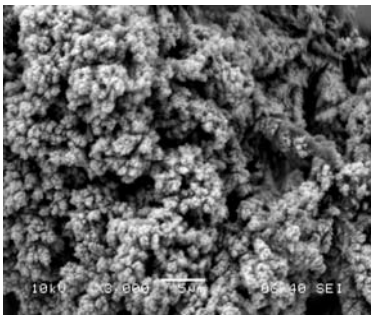
(i)

(120 gl^{-1})

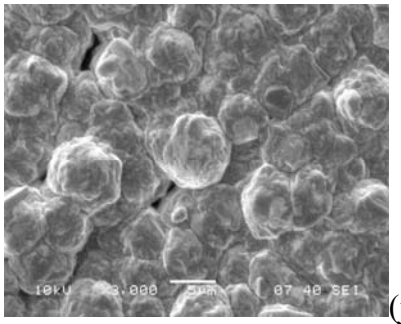
(j)

(Silent)

(Ultrasonic)

Fig-3.11. SEM image of copper deposits at different acid concentration

By applying ultrasound mass transfer is controlled and reduces the dendritic nature of the deposits. So that in low concentration of acid the surface of the deposits looks likes more compact and cauliflower structure than silent condition. By increasing the acid concentration, the surface looks like uniform, pinhole free with spherical grains and the deposits are well covered on the substrate which is shown in fig 3.11. Table 4 shows the compositional EDS analysis of the above discussed deposits. The sonicated deposits are clean deposit, can be inferred from the data.

Table 4. Composition analysis at different acid concentration

	Silent condition				Ultrasonic condition			
Acid conc./Atomic weight%	Cu	O	S	Al	Cu	O	S	Al
40gpl	73.69	26.31	0	0	100	0	0	0
60gpl	71.69	28.31	0	0	100	0	0	0
80gpl	69.16	30.84	0	0	100	0	0	0
100gpl	75.25	20.72	4.03	0	100	0	0	0
120gpl	64.19	30.67	5.13	0	100	0	0	0

3.3. Effect of Copper concentration

3.3.1. XRD analysis

The XRD pattern of the sample synthesized at different copper concentration in silent and ultrasonic condition are shown in fig.3.12 and 3.13.From the XRD analysis it is observed that low intensity peak is observed at $10gl^{-1}$ copper. By increasing the copper concentrations the intensity increases. The peaks in the plane (111), (200), (220) are most prominent than the other peaks. The grain size also increases from31.59nm to 50.14nm by increasing the copper concentration from $10gl^{-1}$ to 50 gl^{-1}.

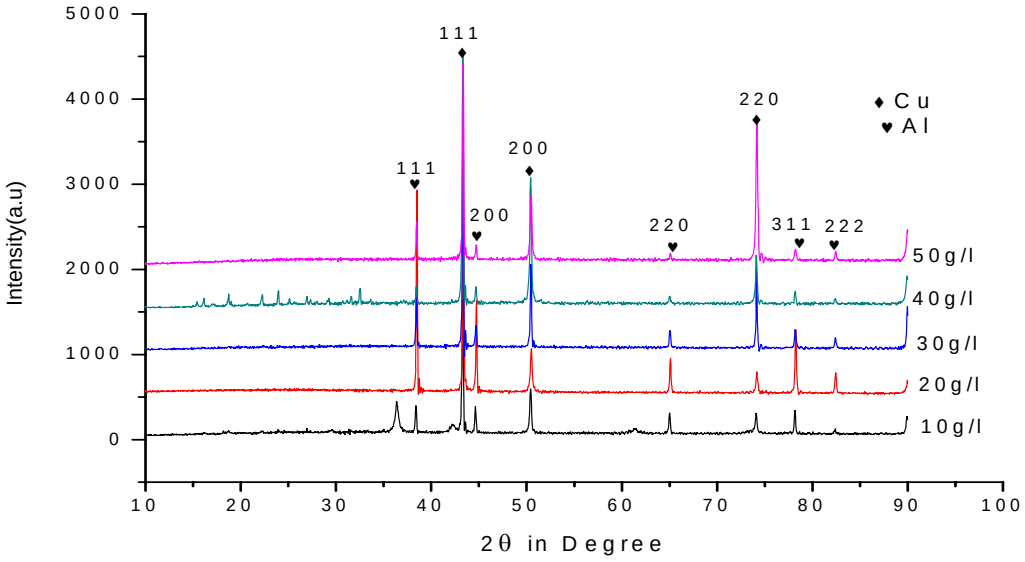

Fig.3.12. XRD patterns of thin film copper electrodeposits at different copper concentrations (silent condition)

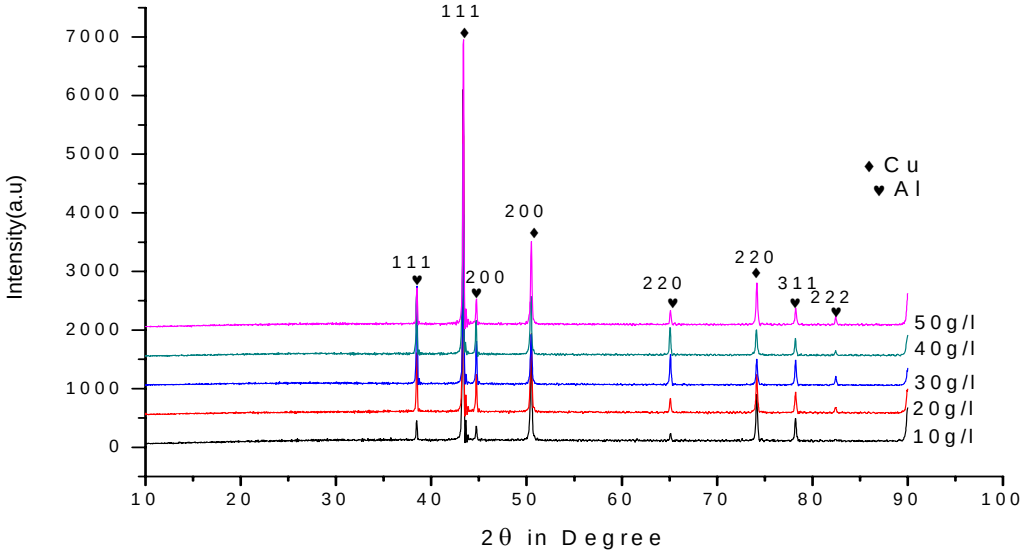

Fig.3.13. XRD patterns of thin film copper electrodeposits at different copper concentrations (ultrasonic condition)

Fig 3.14. Shows the SEM micrographs of copper deposits at different copper concentration in both silent and ultrasonic condition. At low copper concentration the deposit appears to be small dendrites. We believe due to less availability of copper ions the system has become diffusion controlled resulting a mass transfer controlled system leading to dendrite structures in the deposit as shown in fig. 3.14. (a). The corresponding sonicated deposit reveals structure like distorted rose petals. In further increase of concentration the dendrites have become spheroids, the condition of sufficient availability of ions to grow like the SK model as mentioned in chapter 1. With further increase in concentration the substrate has got covered with thin layers of whisker like copper spikes. And at 50 g l^{-1} the ions have arranged themselves to from mushroom like structures. Whereas in presence of ultrasound though the ions didn't get space to move to energy favorable places but have covered the substrate leading to a compact mass. The micrographs also show that for lower copper concentration the nuclei were relatively small and densely distributed on the surface. The EDS compositional analysis is shown in table 5. Unlike the deposits in temperature and acid concentration, it has got oxidized to a less extent. Aluminum is from the substrate material.

Table.5.Composition analysis at different copper concentartion

	Silent condition				Ultrasonic condition			
Copper conc./Atomic weight%	Cu	O	S	Al	Cu	O	S	Al
10gpl	80.71	15.16	4.13	0	100	0	0	0
20gpl	87.17	8.01	0	4.83	100	0	0	0
30gpl	67.29	24.69	5.32	2.70	100	0	0	0
40gpl	49.84	36.91	13.25	0	96.97	3.03	0	0
50gpl	97.09	2.91	0	0	84.91	11.32	0	3.77

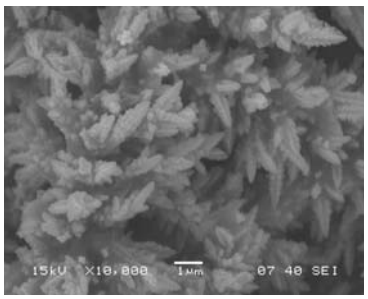

(a) (10 gl^{-1}**)**

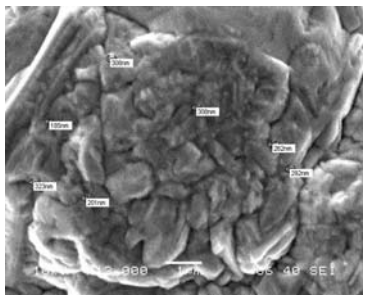

(b)

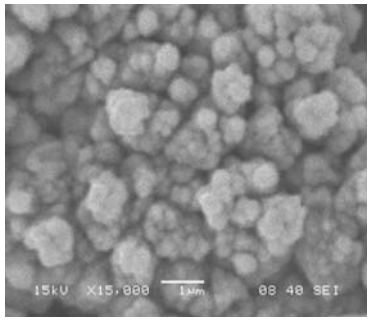

(c) (20 gl^{-1})

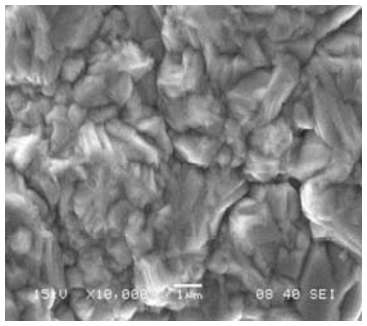

(d)

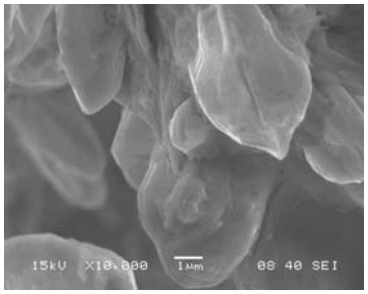

(e) (30 gl^{-1})

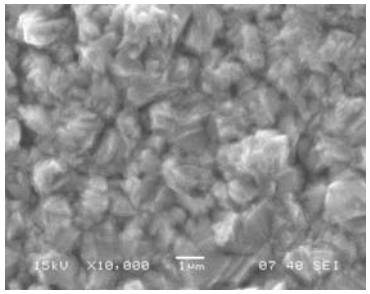

(f)

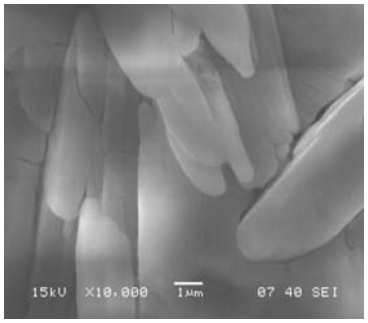

(g) (40 gl^{-1})

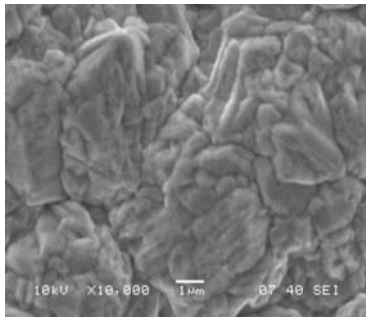

(h)

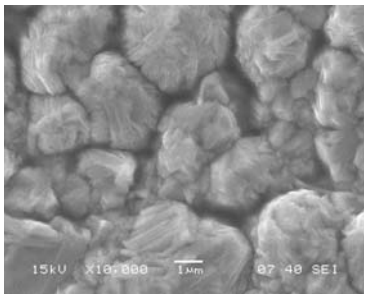

(i) (50 gl^{-1})

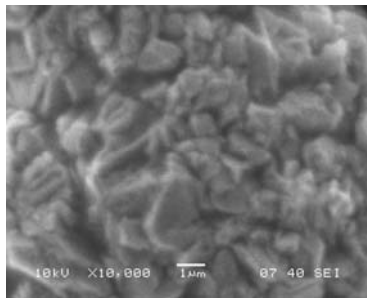

(j)

(Silent) (Ultrasonic)

Fig. 3.14. Copper deposits at different copper concentration

Chapter-4

Conclusion

CHAPTER 4

4. Conclusion

Sonoelectrodeposition is a novel synthesis route for thin film preparation. The deposited film obtained was unique in terms of its morphology and properties. The shape, size, and size distribution of particulates and grains are significantly affected by the reaction condition such as external and internal parameters like temperature, electrolyte concentration, current density, P^H of the solution.The deposited copper thin film obtained at different temperatures illustrates that by decreasing the temperature the grain size reduces because low temperature has resulted high supersaturation favoring formation of smaller nuclei but in a random fashion of discharging. Second**,** ultrasound has helped in rate of mass transportation thus creating enhanced nucleation. This effect has filled the gap between two adjacent nuclei leading to a compact mass. Sonicated deposits are well covered than the silent deposits and hardness of the film increases by decreasing temperature. From the compositional analysis it is confirmed that the percentage of oxygen content of the film increases in silent deposits than sonicated deposition. In low acid concentration the surface is not uniform, the surface film looks like corncob structure but by increasing the acid concentration, the surface looks like uniform means nuclei population density increased but the growth rate is decreased. A specific heat measurement of the above said deposit shows that the heat increases with decreased grain size. The effect of acid concentration in presence of ultrasound shows that the deposits are getting compacted from an open rose like structure to a closed bud structures. The morphology also has similarity to that of the super hydrophobic and adhesive surface of Cassie impregnated wetting state. The deposit is also free from any extraneous impurities because of insitu cleaning of the substrate by ultrasound. A further study in the above mentioned hypothesis may lead to explore some more interesting results. Similarly by increasing the copper concentration the grain size increases due to the increase in metal ions in the electrolyte. In silent conditions the deposit appears to be an agglomerate of numerous copper whiskers. Where as in ultrasonic condition the structures are

fine grained as compared to the silent one. This study supports the fact that ultrasound helps in crystal breakage leading to secondary nucleation.

References

REFERENCES

1. T.Wagner, Thin Film Science, Max-Planck-Institut für Metallforschung, 70174 Stuttgart, Germany, 273(1996)
2. Suryanarayana C. Nanocrystalline Materials, International Materials reviews, Vol 40, No 2 (1995)
3. Chopra K.L. Thin Film Phenomena, Huntingten,Newyork,Robert E.Krieger publishing Company,1979
4. Zhang L., Chen Z., Tang Y, Jia Z. Low temperature cathodic electrodeposition of nanocrystalline zinc oxide thin films, Thin solid films 492 (2005):pp. 24-29
5. Gedanken A. Using sonochemistry for the fabrication of nanomaterials, Ultrasonic sonochemistry,11(2004):pp. 47-55
6. Glocker D. A. , Shah S. Handbook of Thin Film Process Technology, Institute of Physics Publishing, Bristol and Philadelphia, 1998
7. Chopra K.L., Kaur I. Thin Film Device Application,New York &London,Plenum Press,1983
8. Pillai S.O., Solid State Physics, New Delhi,5th Edition,New Age International 2002
9. Mahan John E. Physical Vapor Deposition of Thin Films,New York,Americal vacume society
10. Dobkin D.M.,Zuraw M.K.,Principles of chemical vapour deposition,Kluwer Academic 2003
11. Wagner J.R., Molecular Beam Epitaxy –A simple introduction, university of Michigan 1996
12. Schubert D.W.,Dunkel T.,Spin coating from a molecular point of view, Materials Research Innovation, 7(2003):pp. 314

13. Paunovic M. and Schlesinger M., Fundamentals of Electrochemical Deposition, Wiley, New York, 1998
14. Riley D. Jason, Electrochemistry in nanoparticle science, Current Opinion in Colloid & Interface Science, 7(2002):pp. 186-192
15. Kanani N.,Electroplating-Basic principle,process and practice,Elsevier Ltd.2004
16. James J., Yoreo D., Vekilor Peter.G., Theory of nucleation and growth phenomena,Chapter -3,
17. Budevski E.,Staikov G.,Lorentz W.J., Electrocrystallisation-Nucleation and Growth Phenomena, Electrochimica Acta 45(2000):pp. 2559–2574
18. V.aghavan , Physical metallurgy, principles and practice, New Delhi,Prentice Hall of India Private Ltd.,2006
19. Singh V.,Physical Metallurgy ,1st Edition,Standard Publishers& Distributors,Oct 1999
20. Nanoplating,Film Formation Mechanism in electrodeposition
21. Erdey-Gruz T., Volmer M., Z. Phys. Chem. A 150 (1930): pp.203
22. Volmer M., Weber A., Z. Phys. Chem. 119 (1926):pp. 277
23. Fischer H., Electrochim. Acta 2 (1960):pp. 50.
24. Natter H. and Hempelmann R., Nanocrystalline copper by pulsed electrodeposition: The effects of organic additives, Bath temperature and PH, Vol 50, issue 100(1996): p. 19525-19532
25. Cheng S., Chen G. Chen Y., Huang C, Effect of deposition Potential and bath temperature on the electrodeposition of SnS film, Thin solid film,l 29(2006):pp. 439-444
26. Zainal Z., Kassim A., Hussain m.Z., Ching C., Effect of bath temperature on the electrodeposition of copper tin selenide films from aqueous solution, vol 58,Issue 16,(2004):pp21199-2202
27. Seo M.H., Kim D.J., Kim J.S., The effect of PH and temperature of Ni-Fe-P alloy electrodeposition from a sulfamate bath and the material properties of the deposits, Thin solid films, Vol 489, Issue 12,(Oct 2005):pp. 122-129
28. Lippkow D and Strewhblow H.H., Structural investigation on thin films of copper selenide electrodeposited at elevated temperatures, Electrochimica Acta,Vol 43,No 14-15 (1993):pp.2131-2140
29. Pawer S.M., moholkarA.V.,Bhosale C.H, Materials letter ,61(2007):pp. 1034-1038

30. Dual S.M.S.I,Yun H.J, Shin C.B., Kim C., Electrochimica Acta, 53(2007):pp. 934-943
31. Natter H. and Hempelmann R., *J. Phys. Chem.* 100 (1996), 19525
32. Miskovic V.B., Stankovic M. and Maksimovic M.D., Progress in organic coatings, 16 (1998):p p255-263.
33. Fenineche N. , Chaze A.M., Coddet C., Surface and Coatings Technology 88 (1996) :pp.264-268
34. Scharifker B., Hills G., Electrochim. Acta 28 (7) (1983):pp. 879
35. Grujicic D, Pesic B., Electrodeposition of copper: the nucleation mechanisms, Electrochimica Acta 47 (2002) 2901- 2912
36. Stankovic V.B. and Maksimovic M.D., The effect of concentration on the cathodic Electrodeposition process, Progress in organic coatings,Vol 16 (1998):pp.255-263
37. Cheng Jingquan C and yao Suwei Y.,Rare metals, Synthesis and characterization of silver nanoparticle by sonoelectrodeposition, vol 24, No-4,(Dec 2005) :pp. 376
38. David J Walton, Sonoelectrochemistry-The application of ultrasound to electrochemical systems
39. Chianese A., Contaldi A, Mazzarotta B, J. Crystal Growth 78 (1986) :pp.279
40. Hong Li a,*, Hairong Li b, Zhichao Guo b, Yu Liu b, The application of power ultrasound to reaction crystallization, Ultrasonics Sonochemistry 13 (2006):pp. 359–363
41. Birkin P.R., Silva-martinez S., A study of effect of ultrasound on electrochemical phenomena, ultrasonic sonochemistry,vol 4(1997):pp. 121-122
42. Walker C.T. and Walker R., Effect of ultrasonic agitation on some properties of electrodeposits, Electrodeposition and surface treatment, 1972/73
43. Namgoong E. and Chun J.S., The effect of ultrasonic vibration on hard chromium plating in a modified self-regulating high speed bath, Thin solid film ,l120(1984):pp. 153-159
44. Prasad P.B.S.N.V.,Vasudevan R., Seshadri S.K.,Ahila S., The effect of ultrasonic vibration on nickel electrodeposition, Materials letter, 17(1993):pp.357-359
45. XRD basics,www.scintag.com(last updated 20/04/08)
46. Cullity B.D., Principles of x-ray diffraction
47. Goldstein Joseph I., Scanning electron microscopy and x-ray microanalysis
48. West P., Introduction to Atomic Force Microscopy,Theory,Practice and Application,www.AFMUniversity.org

49. Fischer-Cripps, A.C. Nanoindentation. (Springer: New York), 2004.

50. D. Mott, J. Galkowski, I. Wang, J. Luo, C.J. Zhong, Langmuir, 23 (2007) 5740.

51. Hiroshi Yanagimoto, Kensuke Akamatsu, Kazuo Gotohb, Shigehito Deki, J. Mater. Chem., 11 (2001) 2387.